1 *Ion mobility spectrometry-mass spectrometry (IMS-MS) of small*
2 *molecules: separating and assigning structures to ions*
3
4 **Cris Lapthorn, Frank Pullen* and Babur Z. Chowdhry**
5 *University of Greenwich, School of Science, Medway Campus, Chatham, Kent ME4 4TB, UK*
6 *Frank.Pullen@greenwich.ac.uk*
7

8
9

10 **(ABSTRACT)**
11 *The phenomenon of ion mobility (IM), the movement/transport of charged particles under the*
12 *influence of an electric field, was first observed in the early twentieth Century and harnessed later in*
13 *ion mobility spectrometry (IMS). There have been rapid advances in instrumental design,*
14 *experimental methods and theory together with contributions from computational chemistry and gas-*
15 *phase ion chemistry which have diversified the range of potential applications of contemporary IMS*
16 *techniques. Whilst IMS-mass spectrometry (IMS-MS) has recently been recognized for having*
17 *significant research/applied industrial potential and encompasses multi-/cross-disciplinary areas of*
18 *science, the applications and impact from decades of research are only now beginning to be utilised*
19 *for 'small molecule' species. This review focuses on the application of IMS-MS to 'small molecule'*
20 *species typically used in drug discovery (from 100 to 500 Da) including an assessment of the*
21 *limitations and possibilities of the technique. Potential future developments in instrumental design,*
22 *experimental methods and applications are addressed.*
23
24 *The typical application of IMS-MS in relation to small molecules has been to separate species in fairly*
25 *uniform molecular classes such as mixture analysis, including metabolites. Separation of similar*
26 *species has historically been challenging using IMS as the resolving power, R, has been low (from 3-*
27 *100) and the differences in collision cross-sections that could be measured have been relatively small,*
28 *so instrument and method development has often focused on increasing resolving power. However,*
29 *IMS-MS has a range of other potential applications that are examined in this review where it displays*
30 *unique advantages, including: determination of small molecule structure from drift time, 'small*
31 *molecule' separation in achiral and chiral mixtures, improvement in selectivity, identification of*
32 *carbohydrate isomers, metabonomics, and for understanding the size and shape of small molecules.*
33 *This review provides a broad but selective overview of current literature, concentrating on IMS-MS,*
34 *not solely IMS, and small molecule applications.*
35
36 **Keywords:** ion-mobility mass spectrometry; ion mobility spectrometry; mass spectrometry; small
37 molecule; mass-mobility correlation; collision cross-section; ion mobility; FAIMS; drift-time; travelling
38 wave; structural; computational; differential mobility spectrometry; differential mobility analyzer
39

40 **I. INTRODUCTION TO IMS**
41 The existence of ions in the gas-phase was first discovered when investigating changes in the
42 electrical conductance of air (Thomson, 1903) which had previously been thought to be an electrical
43 insulator. Further work established the generation of ions by UV and X-ray from work by Thomson and
44 Rutherford (1896), Roentgen (1896) and Rutherford (1897)). The rudimentary scientific tools available
45 at the time did not allow a comprehensive understanding of ion behaviour but the behaviour of simple
46 gas-phase ions in a weak electric field was further elucidated by Langevin (1905), who demonstrated

47 that air was a mixture of gases and developed models that described these simpler systems
48 remarkably well.
49
50 Thomson and Aston later developed the first mass spectrometer (Aston, 1919) and further research
51 focussed on low pressure studies of ion-molecule systems that, although not directly involving typical
52 ion mobility pressure regimes, accrued knowledge in the behaviour of ion motion in a partial vacuum.
53
54 The rapid uptake of IMS in military and forensic applications (Zolotov, 2006) benefited from the
55 relatively high proton affinity of the analytes (chemical warfare agents, explosives and illicit drugs),
56 low detection limits and miniaturisation of IMS instrumentation. IMS instrumentation was re-designed
57 for the field, used internal calibrant standards and simplified user interfaces allowed their use by non-
58 scientist military and security personnel. IMS instrumentation is now ubiquitous in handheld forensics,
59 cleaning validation and military applications (from border control to explosive testing in war zones).
60
61 Separation in IMS occurs rapidly, in milliseconds, rather than seconds as in chromatography, so IMS
62 is now beginning to be recognised as a powerful separation step which can be utilised post-ionisation
63 using a range of equipment, benefits from robust day-to-day operation and allows size and shape
64 separation and measurement of analytes that cannot easily be derived using other techniques.
65 Miniaturisation, demonstrated so far primarily in overtone IMS and microfabricated Field Asymmetric
66 IMS (FAIMS), is a highly attractive feature and IMS typically has a low detection limit of nanograms
67 and does not require expensive and environmentally damaging solvents.

II. INTRODUCTION TO IMS-MS

69 The most important aspect of the combination of an IMS separation (typically occurring in the
70 millisecond time-frame) and MS detection (typically occuring in the microsecond time-frame) is that it
71 allows an additional separation step to be obtained on a MS time-frame (e.g. in addition to liquid
72 chromatography), without compromising the speed of MS detection.
73
74 The work of McDaniel and Martin (1960), Kebarle (1965) and Hogg (1965), Albritton et al., (1968) and
75 later Crompton and Milloy (1977) developed the recognizable configuration of linear drift-tube IMS
76 (DT-IMS). The combination of ion mobility and mass spectrometry allowed more complex studies to
77 be conducted in order to develop models of ion mobility.
78
79 IMS was first hyphenated to a mass spectrometer by Barnes, McDaniel and Martin (1961) using a
80 magnetic sector mass spectrometer; subsequently McAffee and Edelson (1963) described
81 hyphenation to a time-of-flight (TOF) MS. The coupling of IMS with a TOF mass spectrometer is
82 particularly appropriate because the TOF mass spectrometer has the fastest data acquisition rate of
83 any mass spectrometer and can acquire many spectra on the microsecond scale whilst the IMS
84 analytes arrive on a millisecond timescale.
85
86 A review by Hill et al. (2007) describes the early development of IMS-MS with significant contributions
87 and discoveries including those from Bowers, Kemper, Clemmer and Kebarle. IMS has since been
88 interfaced to quadrupole mass spectrometers (Karasek et al., 1976; Wu et al., 1998), quadrupole ion
89 traps (Creaser et al., 2000), linear ion traps and Fourier-transform ion cyclotron mass spectrometers
90 (Bluhm et al., 2000) which is beneficial in terms of a wider linear dynamic range and increased mass
91 spectral resolution. Clemmer et al., (1997) and Creaser et al., (2000) also reversed the stages to
92 produce a MS-IMS design that traps and stores ions in an initial quadrupole ion trap for subsequent
93 ion mobility measurements which has the advantage of pre-concentrating low abundant components.
94
95 Recently IMS has been hyphenated to mass spectrometry systems and the availability of
96 commercially supported instrumentation has arguably led to a rapid increase in the number of
97 publications on IMS-MS, as shown in FIGURE 1. FAIMS, a type of differential mobility spectrometry,
98 originated in Russia in the early 1980s (Gorshkov, 1982) emerged as an analytical tool (Buryakov et
99 al., 1993), and was later commercialised by Ionalytics (Selectra, 2003), as a front-end accessory for
100 MDS Sciex (Concord, Ontario, Canada) mass spectrometer systems (2004), Thermo FAIMS, (2007)
101 and Owlstone Nanotechnologies FAIMS. Waters Inc. (Milford, MA) launched the first generation Synapt
102 Triwave travelling wave IMS system in 2006 and updated with a second generation instrument with
103 improved resolution (G2, 2009) and improvements to sensitivity (G2S, 2011). AB Sciex launched the

104 SelexION ion mobility device in 2011 for their triple quadrupole mass spectrometer and quadrupole-
105 trap mass spectrometer.
106
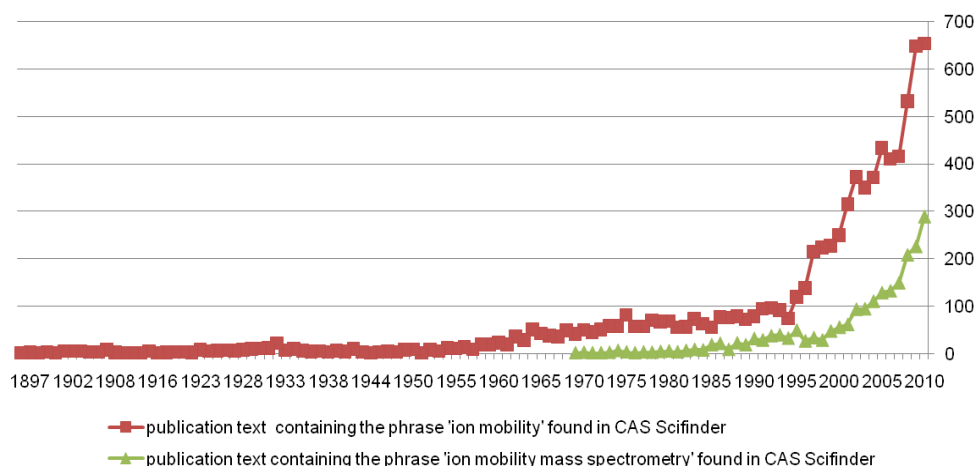
107
108 **FIGURE 1.** Chart showing number of publications containing the phrases "ion mobility" and "ion
109 mobility mass spectrometry" obtained using CAS Scifinder.

110
111 There has been limited recognition of the potential of IMS-MS analysis for 'rule-of-5' type small-
112 molecules (Lipinski et al., 1997) outside of traditional IMS analyte classes (e.g. explosives, chemical
113 warfare and illicit drugs). The historical lack of interest and sporadic periods of development in IMS-
114 MS for small molecule applications seems most likely to be due to perceived poor resolution,
115 strengths in competing chromatographic techniques and weaknesses in the robustness of IMS
116 regarding a poor linear range (Turner and Brokenshire, 1994), "memory effects" from contamination
117 (Gehrke, 2001) and interference from matrices.

118
119 In contrast IMS-MS has been applied to biomolecules including peptides (Harvey, Macphee & Barran ,
120 2011), proteins (60 kDa-150 kDa) and large protein complexes (1- 4 MDa) (Uetrecht et al., 2010)
121 particularly after the application of non-covalent mass spectrometry conditions to IMS-MS. Using
122 these especially gentle electrospray ionisation conditions is believed to maintain the weak
123 (cooperative) molecular interactions present in many biomolecular structures and thus avoid
124 fragmentation. Whilst IMS-MS typically lacks the resolution (1% error or 10 nm^2) of x-ray or NMR for
125 large molecular weight biomolecules it enables analysis using smaller amount of material, allows
126 analysis of structures >100 kDa that are difficult to analyse by NMR and is, arguably, as realistic an
127 environment as x-ray structures due to lattice effects present. IMS-MS has, therefore, been utilised as
128 a tool to probe the stabilisation of proteins in the presence of ligands and metals (as a unique method
129 of metal speciation; Souza Pessôa et al., 2011), protein-protein-interactions, protein mutants and their
130 structural consequences as well as protein unfolding via various means of ion activation (Jurneczko
131 and Barran, 2011). In addition to detailed understanding of individual biomolecular systems, IMS-MS
132 has also been applied to more high-throughput analytical approaches including screening of
133 phosphorylated peptides (Thalassinos et al., 2009), identification and separation of chemically cross-
134 linked peptides (Santos et al., 2010) and combining topology in protein substructures with proteomics
135 data (Zhou and Robinson, 2010). This review does not attempt to summarise biomolecule analysis by
136 IMS-MS, which is covered by many authors, but rather to contrast the adoption of IMS-MS in
137 biomolecule analysis and focuses on small molecule applications.

138 ## III. DIFFERENCES IN PERFORMANCE OF IMS-MS AND IMS

139 ### A. The ion efficiency and resolution challenge
140 Some of the key differences between IMS and hyphenated IMS-MS include the pressure regime in
141 the ion mobility cell, the size of the instrument and the typical ionisation source. Whilst specifications
142 and performance in IMS may be indicative of those in IMS-MS there are some technical reasons why
143 this may not follow. It is critical to note that the results may well be different in IMS-MS compared to
144 IMS especially due to sensitivity issues and pressure regime changes from IMS to MS stages.
145

146 In IMS-MS there are often two main challenges (i) to utilise all the ions from the ionisation source,
147 (especially in a pulsed IMS separation such as drift-time IMS, but not a challenge in DMS or FAIMS
148 which typically have a 100% duty cycle if a single transmission voltage is selected) and (ii) elimination
149 of all neutral species whilst ensuring transmission of ions to the MS stages to maintain sensitivity.
150 Traditionally DT-IMS-MS sensitivity has been estimated to be inversely proportional to the IMS
151 resolving power squared; ion losses at the IMS exit aperture ranging from 99 to 99.9% (Tang et al.,
152 2005) and ion introduction losses being between 99.6 to 99.9% (Belov et al., 2008). The desire to
153 increase the gas pressure in the DT-IMS cell to increase resolution must therefore be balanced with
154 the possibility that it may well reduce ion transmission by requiring a reduction of the aperture size in
155 the interface from IMS to MS. The different pressure regimes in IMS systems are described in Table 1.
156
157 For DT-IMS-MS the drift gas pressure must be increased proportionally to electric field strength in
158 order to maintain a low E/N ratio (<2 x 10^{-17} Vcm^2), required to obtain field-independent mobilities for
159 which the simplified Mason-Schamp equation (Mason and McDaniel, 1988) holds:
160
161
162 $$K = (3q/16N)(2\pi/\mu kT)^{1/2} 1/\Omega \qquad (1)$$
163
164
165 Where K is the ion mobility, q is the ionic charge, N is the buffer gas density, μ is the reduced mass
166 of the buffer gas and the ion, k is the Boltzman constant, T is the temperature and Ω is the collision
167 cross-section (CCS).
168
169 For Travelling Wave Ion Mobility-MS (TWIMS-MS) the gas pressure must also be increased
170 proportionally to the electric field, such that:
171
172
173
174
175 $$K = K_o N_o / N = K P_o T / (P T_o) \qquad (2)$$
176 where K is the ion mobility, N is the buffer gas density, N_o is the Loschmidt number (the value of N
177 at standard temperature (T_o = 273K) and pressure (P = 1 Atm) and K_o is the reduced ion mobility.
178
179 **TABLE 1**. Pressure regimes in typical IMS systems.
180

Type of IMS system	Pressure regime	Typical operating pressure
Ambient DT-IMS	Ambient pressure	1000 mbar (Kanu et al., 2008)
Reduced pressure DT-IMS	Reduced pressure	10^{-5} (Ruotolo et al., 2002b) to 1.3 (Valentine et al., 2001) mbar
FAIMS or DMS	Ambient pressure->ambient pressure	400 to 1571 mbar (Kolakowski and Mester, 2007)
Travelling wave IMS	Reduced pressure	0.5 mbar (Waters Synapt G1) to >3 mbar (Waters Synapt G2) (Giles et al., 2011)
Differential mobility analysis	Ambient pressure	1013 mbar

181
182 Approaches to maximise sensitivity include utilising quadrupole and octopole ion traps (Henderson et
183 al., 1999;Creaser et al., 2000; Myung et al., 2003) and electrodynamic ion funnels (Wyttenbach et al.,
184 2001) to accumulate and introduce ions efficiently from the ion source to increase the sensitivity of
185 DT-IMS. Multiplexing approaches including Hadamard (Clowers et al., 2006) and Fourier-type (Tarver,
186 2004) gating techniques have also been utilised for increasing the sensitivity of DTIMS, by increasing
187 the frequency of ion injection events and thus increasing the quantity of ions injected into DT-IMS by
188 up to 50%. Most of these approaches have been integrated into full IMS-MS systems with dramatic
189 improvements in sensitivity.
190
191 There is some uncertainty in the identification of the ions in their transmission through the IM cell and
192 it seems clear that hyphenating IMS and MS allows a more comprehensive understanding of the

193 ionisation processes and fragmentation pathways in IMS. For example, when using a radioactive ^{63}Ni
194 cell, proton transfer to the analytes should lead to protonated monomer and dimer ions; however,
195 without a mass spectrometer as the detector, the identification of the ions in the ion cell cannot be
196 unambiguously ascertained. Indeed, a comparison of limonene and 2-nonanone by IMS and IMS-MS
197 resulted in a variety of unexpected fragments and ions, resulting in a non-trivial IMS spectrum and
198 making interpretation of the results difficult (Vautz et al., 2010). Any unambiguous identification of ions
199 in IMS will be important both in structural measurements (size, shape and topology) and for
200 comparison of related IMS techniques (e.g. TWIMS-MS) that often use historical DT-IMS-MS data as
201 calibration standards in ion mobility and collision cross-section calculations.

B. Features of IMS techniques utilised in IMS-MS

203 IMS-MS potentially provides a number of advantages over and above IMS including:
204   i) as a rapid gas-phase separation step before mass spectrometryanalysis,
205   ii) the identification of ions subsequent to characteristic drift times by comparison with data
206   acquired under comparable conditions,
207   iii) measurements of collision cross-sections and derivation of further information about size and
208   shape, either by comparison with computational modeling or by analysis within a series of
209   compounds
210 iv)   better characterisation of ion and ion-neutral ion mobilities by simultaneous acquisition of
211   mass spectrometry data, and
212 v)   better characterisation of ionisation (Tang et al., 2006) and fragmentation pathways via a
213   better understanding of gas-phase ion structures

215 IMS has been hyphenated to liquid chromatography, gas chromatography (Baim and Hill, 1982;
216 Snyder et al., 1993), super-critical fluid chromatography (Eatherton et al., 1986; Huang et al., 1991),
217 ions produced via matrix assisted laser desorption ionisation (Jackson et al., 2007), desorption
218 electrospray ionisation (Weston et al., 2005), pulsed corona discharge ionisation (Hill and Thomas,
219 2003) and miniaturised to microchip scale (Shvartsburg et al., 2009b).

221 IMS-MS systems are typically composed of four stages (Figure 2):
222   1) an ion source e.g. MALDI or electrospray that generates ions. Electrospray ion sources have
223   been preferred for retaining native-like structures in biological systems.
224   2) an IMS cell, where charged particles migrate under the influence of an electric field.
225   3) a mass analyzer, typically a time-of-flight (TOF) mass spectrometer which is designed to
226   allow a fast acquisition rate and large mass detection range.
227   4) an ion detector.
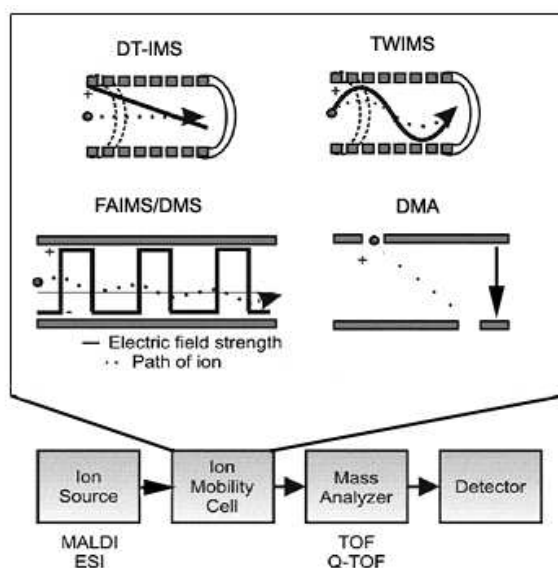
230 **FIGURE 2.** Overview of typical ion-mobility mass spectrometer configurations, adapted from Enders
231 and Mclean, 2009.

232 There are four main types of IM cell utilised in IMS-MS.
233 (i)　　Drift-time IMS (DT-IMS) is the simplest configuration where collision cross-section (CCS) can
234 　　　be directly calculated without calibration and provides the highest resolving power. A tube is
235 　　　filled with a buffer gas (or mixture) and a low voltage field is applied, typically from 5 to 100
236 　　　Vcm^{-1}. The ions collide with neutral buffer gas molecules, exit via a detector and the collision
237 　　　cross-section Ω_T, at a temperature T can be obtained by measuring the velocity of the ions
238 　　　and solving the Mason-Schamp equations at intermediate electrical fields (5-100 Vcm^{-1}):
240

$$V_d = KE \tag{3}$$

242 where v_d is the drift velocity of the ion, K is the ion mobility, E is the imposed electric field,
244 and

$$\Omega_T = \left(\frac{3ze}{16N} \right) \left(\frac{2\pi}{\mu kT} \right)^{1/2} \left(\frac{1}{K} \right) \tag{4}$$

246
247 where z is the numerical charge, e is the elementary charge, N is the number density of the
248 buffer gas, μ is the reduced mass of the ion- buffer gas neutral pair, k is the Boltzmann
249 constant and T the temperature in Kelvin.
250
251 DT-IMS suffers from an inherent lack of sensitivity, due to a pulsed analysis (where ions are
252 measured in packets), and the subsequent loss in duty cycle, as the time between packets of
253 ions is not utilised. A review of IMS by Eiceman and Karpas (2004) discusses the history of
254 IMS, the chemistry and physics of ion behaviour and reflects on the potential future
255 development and applications of IMS.
256
257 In linear DT-IMS, illustrated in FIGURE 3, the sample is introduced to an ionisation region
258 where ionisation can take place by a number of methods including β-emission from a [63]Ni
259 corona discharge, photo-ionisation, electrospray etc. Ions are allowed through an electric
260 shutter grid, whilst neutrals remain in the ionisation source and the measurement time is
261 initiated. The drift tube can vary in length from 5 centimetres to 3 metres or more. An electric
262 field gradient, typically from 10-100 Vcm^{-1}, from the ionisation source to the detector causes
263 the ions to traverse the drift tube at a constant velocity.　A drift gas is introduced counter-
264 current to the flow of ions keeping the drift-tube free of neutrals which could participate in ion-
265 neutral clusters.
266

Ionization region　　　　　　　　*Drift region*　　　　　　*Detector*
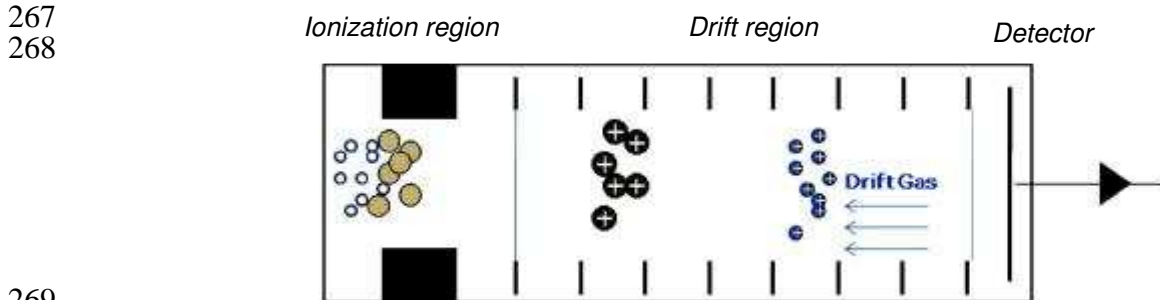
270 **FIGURE 3.**　Illustration of DT-IMS, adapted from Eiceman and Karpas (2004).　A voltage
271 gradient is applied to the ions from left to right.

273 The total ion signal is detected and plotted with respect to time to form an ion mobility
274 spectrum, e.g. (see FIGURE 4) for a mixture of amphetamines analysed by ESI-DT-IMS-MS
275 (Matz and Hill, 2002). Smaller ions travel faster through the drift region and have shorter drift
276 times, compared to higher molecular weight ions that drift slower and possess longer drift
277 times.

279
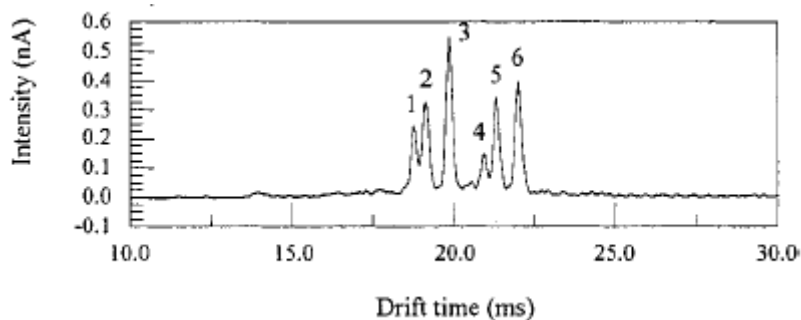
FIGURE 4. ESI-DT-IMS-MS spectrum of a mixture of 1) amphetamine, 2) methamphetamine, 3) ethylamphetamine, 4) 3,4-methyldioxyamphetamine, 5) 3,4-methylenedioxy methamphetamine and 6) 3,4-methylenedioxyethylamphetamine, adapted from Matz and Hill (2002a).

Another complementary approach to classical DT-IMS-MS was the use of the second quadrupole (Figure 5) in a triple-quadrupole mass spectrometer as an ion mobility device; while this approach was never commercialized it did open up opportunities in hyphenation of IMS and MS. In the triple quadrupole energy loss method an incident ion is transmitted to the second quadrupole of a triple quadrupole mass spectrometer where the ion will experience a drag coefficient and generate a stopping curve; from the stopping curve the ion mobility can be measured and a collision cross-section determined. Indeed, Covey and Douglas (1993) were the first to measure collision cross- sections for some biomolecules using this method and also later reviewed collision dynamics in quadrupole systems including an assessment of the internal energy of the $C_6H_5^+$ ion by measuring the increase in collision cross-section after collisional activation (Douglas, 1998) .

293
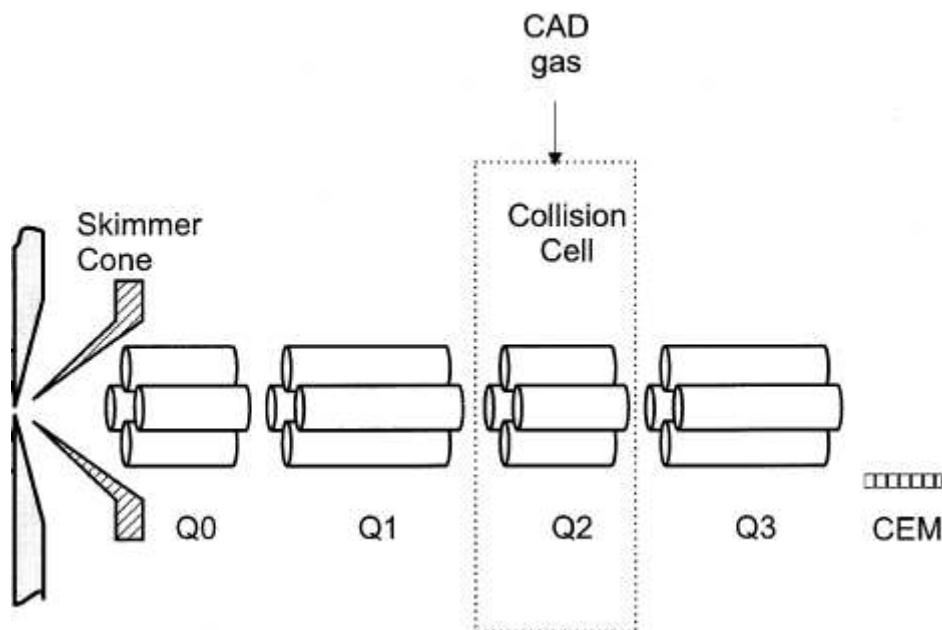
FIGURE 5. Schematic of the triple quadrupole configuration that can be used to obtain ion mobility measurements via an energy loss method, adapted from Purves et al. (2000).

This triple-quadrupole energy loss method was further developed to utilise segmented collision cell rods separated by small 1 mm gaps that enabled a radio-frequency only quadrupole drift cell to be used to reduce ion losses due to diffusion and enable mass selection before or after the drift cell, and a DC gradient that moved the ions in an axial direction (see Figure 6, Javahery & Thomson, 1997). Unfortunately this configuration was outside the typical low-field IMS range and may have resulted in field-heating of ions. This configuration was later improved to possess an increased gas pressure and lower field concentration that resulted in minimal internal excitation of the ions (Guo et al. 2004).
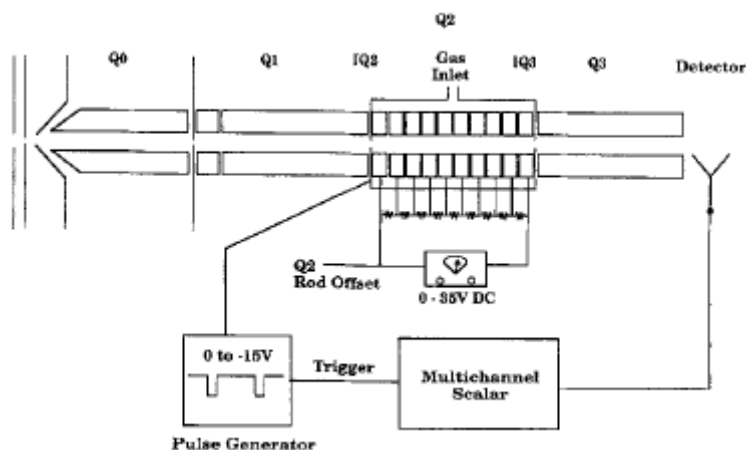
FIGURE 6. Schematic of a segmented triple quadrupole configuration that can be used to obtain ion mobility measurements, adapted from Javahery & Thomson (1997).

(ii)   Differential mobility IMS (DMS) or FAIMS uses a sequence of intermediate and high field regimes where the behaviour of ions is described empirically by the Mason-Schamp equation (Mason and McDaniel, 1988) under a high-field regime, which can be expanded to an infinite series of E/N:

$$K_0(E) = K_0(1 + a(E/N)^2 + b(E/N)^4 + c(E/N)^6 + ...) \tag{5}$$

where K_0 is the reduced ion mobility, E is the field intensity and N is the buffer gas number density. However, under a typical FAIMS electric field the mobility can be approximated by using the first two factors as the importance of the sixth order and higher are insignificant (the fourth order is two orders of magnitude smaller than second order, and the second order is three to five orders of magnitude smaller than one (see Shvartsburg et al., 2004).

The basic principle of operation is that ions are introduced to a region with electrodes and a stream of gas acts as a transport medium. An asymmetric waveform is passed across the electrodes, which consists of a high potential electric field for a short time followed by a low potential electric field for a longer time; this typically fixed dispersion voltage (DV) waveform is superimposed with a variable compensation voltage (CV) to maintain a stable trajectory for the analyte ion. This process will effectively select ions and act as an ion filter, as shown in Figure 7. A cylindrical electrode configuration has usually been designated FAIMS, whereas parallel plate configurations have typically been designated as DMS.

336
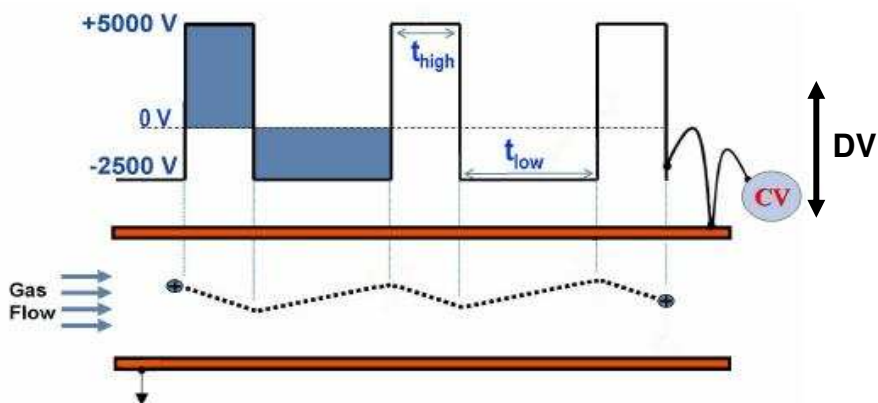
FIGURE 7. Illustration of an example of a parallel plate DMS with compensation voltage applied showing ion transmission, adapted from Thermo Fisher Scientific Inc., FAIMS Operators manual (2007).

A compensation voltage scan measurement (Figure 8) shows a typical profile attained by optimising the effect of inner and outer electrode temperatures on peak profile for morphine and its 3-β-D-glucuronide metabolite (Hatsis et al., 2007). Optimising the separation of morphine whilst maintaining sensitivity was reported to enable the metabolite interference to be effectively filtered out, and significantly improve the quantification of morphine.

346
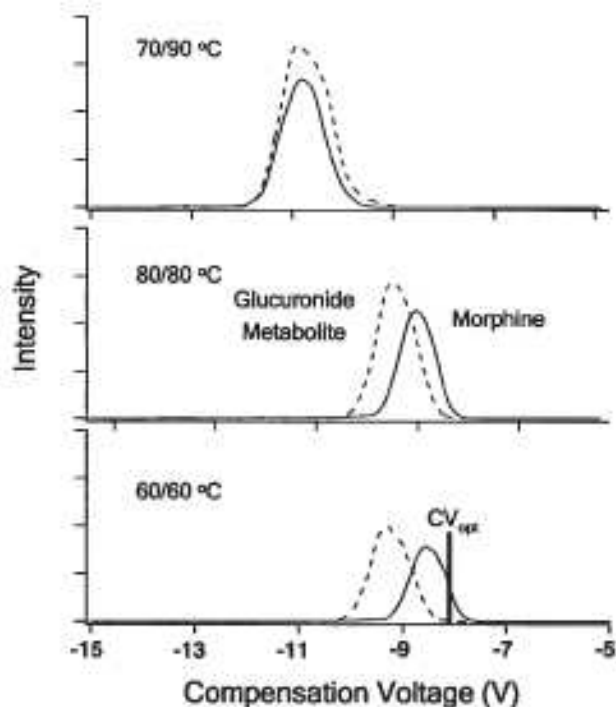
FIGURE 8. Compensation voltage scans of morphine and the glucoronide metabolite, adapted from Hatsis et al., (2007).

The use of compensation voltage optimisation to select an analyte ion can result in a clear difference in the mass spectrum observed resulting in an increased S:N ratio for the analyte and a reduction in other signals as shown in the use of ESI-FAIMS-MS with cisplatin and its hydrolysis products (Cui et al., 2003) shown in FIGURE 9.
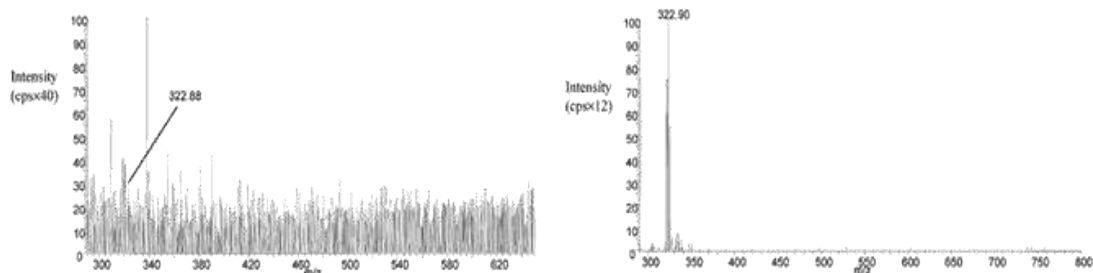
FIGURE 9. Mass spectra showing the reduction in background noise from (a) ESI-MS to (b) ESI-FAIMS-MS, adapted from Cui et al. (2003).

Currently the factors determining the separation mechanism in FAIMS or DMS and factors governing peak width as well as transmission remain relatively difficult to predict (Shvartsburg et al., 2004). The parameters influencing performance include field intensity, ion path length, gas properties (composition, temperature, pressure), shape and width of electrodes, the profile and frequency of asymmetric waveform, compensation voltage scan speed and gas flow. Champarnaud et al., (2009) studied the separation of trace level impurities by combining experimental observation with a Design of Experiment (DOE) statistical treatment that indicated important factors in the optimisation of the values of the compensation voltage, signal intensity, separation, peak asymmetry and peak width. However, a study of tetraalkylammonium ions found standard conditions were often suitable for selecting ions with an m/z value of 100-700 (Aksenov and Kapron, 2010). The simulation of ion motion in planar electrode FAIMS and cylindrical electrode FAIMS, provided insights into design, experimental variables and interpretation (Smith et al., 2009b) and some of the key molecular and instrumental parameters affecting performance were discussed by Nazarov (2006) and Levin et al. (2004).

Whilst there are several novel geometries (Prieto, 2011), there are two main forms of field asymmetrical waveform ion mobility spectrometers: 1) those with planar electrode geometry and 2) those with curved electrode geometry. Both planar geometry and the curved geometries of FAIMS and DMS evolved during the 1990s, and in the early 1990s the term differential mobility spectrometry (DMS) became generally synonymous with planar electrodes and the term FAIMS became synonymous with curved geometries, although there are multiple examples of overlapping usage of the terms DMS and FAIMS. One of the primary differences relates to the use of polar transport gas modifiers. Planar devices create homogeneous electric fields which enables the use of transport gas modifiers without resolution losses whereas curved geometries tend to create inhomogeneous fields which lead to a loss in resolution when using transport gas modifiers. However, curved geometries have been shown to provide some degree of ion focusing at atmospheric pressure resulting in higher sensitivity (Guevremont & Purves, 1999; Krylov, 1999). Planar line-of-sight analyzers enjoy the convenience of transmitting all ions when the RF voltages are turned off, so that operation without mobility separation can be achieved simply by turning off the fields. Curved geometry/non line-of-sight FAIMS require the device to be removed for operation without mobility separation. A wider analysis of the differences between alternative geometries was described by Krylov (2003).

A comprehensive review discussed the applications of FAIMS for drinking water analysis, pharmaceutical metabolite identification and separation of isomers and isobaric peaks (Kolakowski and Mester, 2007). In addition a detailed account of the fundamentals of DMS and FAIMS has been written by Shvartsburg (Shvartsburg, 2010).

(iii)   Travelling wave ion mobility spectrometry (TWIMS) is a novel method whereby ions are separated according to their mobility in a series of voltage pulses in a travelling wave (T-wave) mobility cell utilising RF ion guides (Gerlich, 1993). The resolving power is relatively low; however, collision cross-sections can be derived by calibration with known standards. This ion mobility approach has been successfully interfaced to a conventional time of flight mass spectrometer and, due to the trapping gates and fast data acquisition rate of the TOF, good sensitivity is achieved. Despite attempts (Shvartsburg and Smith, 2008; Smith et al., 2009a)

405 the motion of ions in TWIMS is not fully understood and TWIMS calibration is typically used to
406 calculate CCS values. The commercial technical and software support has arguably
407 reinforced attempts to utilise IMS-MS in separation, characterization and measurement
408 applications, for example, via the routine use of multidimensional data in Driftscope software
409 (Williams et al., 2009a) and software to process complex data such as time-aligned parallel
410 fragmentation (D'Agostino and Chenier, 2010).
411
412 In travelling wave ion mobility spectrometry a transient DC voltage pulse is applied in order to
413 create an electromotive force via a series of sequentially opposite polarity RF-only rings to
414 create a travelling wave which propels ions through the device, as shown in Figure 10. Ions
415 with high ion mobility slip behind the wave less often (or spend more time surfing) than ions of
416 low ion mobility thus enabling separation based on relative ion mobility.
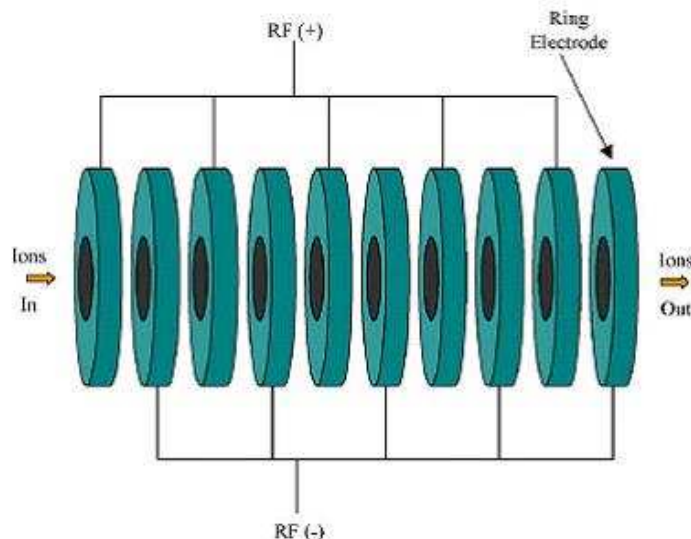
417
418 **FIGURE 10.** Illustration of a stacked ring ion guide used in traveling wave ion mobility spectrometry
419 (TWIMS), adapted from Pringle et al. (2007).

420
421 Visualising data obtained using the proprietary Driftscope software enables a range of options
422 for understanding the data including 3D visualisation, 2D plots and intensity views etc, The
423 data can be interactively processed if desired, for example, to show data that only contains a
424 certain component using various geometric selection tools such as lasso and square area.
425
426
427 (iv) The Differential Mobility Analyser (DMA) was originally developed to generate particles in
428 order to calibrate aerosol instruments, later expanded to describe the mobility of non-diffusing
429 particles by Knutson and Whitby (1975) and recently to describe the mobility of diffusing
430 particles by Stolzenberg & McMurray (2008). The DMA consists of a combination of electric
431 field mobility in addition to a fast gas stream, only ions with a well defined electrical mobility
432 are transmitted into an outlet slit leading to the mass spectrometer inlet (see Figure 11). The
433 DMA vacuum regime means that the measured ions do not experience a vacuum interface or
434 ion guide so may be less prone to structural modifications (Hogan et al., 2011) and, as the
435 separation technique is a space-dispersion rather than a time-dispersion technique, the ions
436 can be continuously transmitted to a mass spectrometer.
437
438
439

440
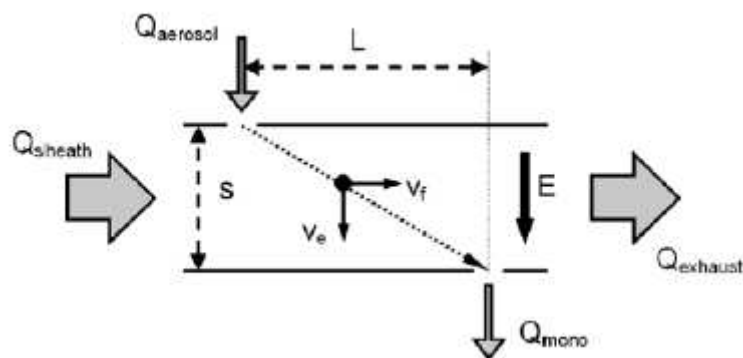
FIGURE 11. Schematic of the operation of a differential mobility analyzer. Ion are injected at the top left and move downwards and to the right, over a distance S, under the influence of an electric field E, adapted from de la Mora et al., (2006)

The DMA technique may be considered a hybrid of DT-IMS and DMS as the separation process is based on the low electric field mobility like DT-IMS, however the sampling is continuous as in DMS. DMA-MS has been most widely explored for large molecules; however, discussion on multiple charged polyethylene glycol ions (Ude et al. 2004) illuminated structures from approximately 300 Da to 3000 Da describing configurations for long straight chain molecules. One of the advantages of DMA is that it can, theoretically, be easily added to existing mass spectrometry stages without complex interfaces due to operation at atmospheric pressure (Rus et al., 2010). A DMA was coupled to an existing Sciex QStar MS (Concord, ON, Canada) enabling separation of L-alanine and an isomer, sarcosine, (Martínez-Lozano P et al., 2010) which are proposed to be small molecule biomarkers from urine in the progress of prostate cancer.

IMS covers a range of different techniques and unfortunately some gross simplifications have resulted in terminology that may be confusing.
1. DTIMS is also known as Classical IMS, Conventional IMS, Standard IMS, Drift-Tube IMS, Time of flight IMS, Traditional IMS, Plasma Chromatography and Ion Chromatography.
2. DMS includes High Field Asymmetric Waveform IMS (FAIMS), Field Ion Spectrometry and Ion mobility Spectroscopy and is commercialised in the Ionalytics Selectra, Thermo FAIMS, Owlstone Nanotechnologies and AB Sciex Selectra systems.
3. Travelling wave ion mobility spectrometry (TWIMS) is commercialised in the Waters Synapt systems.
4. Differential Mobility Analysers (DMA) have been developed by several groups at Yale (USA), CIEMAT (Madrid) and RAMEM (Madrid).

Comparison of key benefits and challenges of IMS-MS methods
There is currently a wealth of IMS-MS systems available both commercially and being used and developed in academic institutions.

DT-IMS-MS has been most widely used in academic institutions and provided some of the highest resolving powers. An advantage of DT-IMS-MS is that the ion mobility can be determined experimentally and collision cross section determined without requiring calibration. A key challenge is that the pulsed analysis leads to an inherent loss of duty cycle and hence reduction in sensitivity.

An advantage of both DMS-MS and FAIMS-MS is that it operates as a continuous device when the compensation voltage is selected so does not have the 'lossy' sampling issues of DT-IMS and TWIMS. The separation appears to be orthogonal to m/z and sometimes size so that separations may be uniquely tuned to select a chosen analyte and thus be used as a powerful separation technique. A key challenge is that it has proven difficult to definitively assign structural properties and changes to DMS measurements as several factors appear to contribute to the clustering/declustering mechanism and analyte drift times thus it appears to be best utilized as a separation device.

An advantage of TWIMS-MS is that it is commercially supported and that the ion mobility can be determined experimentally and collision cross-section determined with suitable calibration. Whilst the

487 resolution obtained in TWIMS is typically lower than dedicated DT-IMS-MS and some FAIMS/DMS
488 the software to interpret and process the complex data is well supported.
489
490 Advantages of DMA-MS include operation in the low electric field regime that typically means less
491 structural distortions and determination of collision cross-section, a continuous sampling rate that
492 should mitigate sensitivity losses (with reported transmission efficiencies of up to 50% (Martínez-
493 Lozano et al., 2011)) and the theoretical ability to add the device as a front-end to many existing mass
494 spectrometer systems. However DMA-MS has not been fully commercialized yet or utilized for the
495 multitude of "small molecule" applications explored in DT-IMS-MS, FAIMS-MS, DMS-MS and TWIMS-
496 MS though it shows significant promise.

497 **C. Understanding IMS-MS resolving power and selectivity**
498 IMS can separate analytes based on their ion mobility including closely related species such as
499 isomers (Williams et al., 2010), isobars and isotopomers (Shvartsburg et al., 2010a). The key
500 parameters affecting a useful separation are 1) the resolving power and 2) the selectivity.
501
502 **Resolution and peak capacity in IMS**
503 The combination of ion mobility and mass spectrometry in IMS-MS offers a technique that is able to
504 distinguish components based on their size to charge ratio (Ω/z for IMS) and mass to charge ratio
505 (m/z for MS), thereby enabling orthogonal specificity. Even with expensive high-resolution mass
506 spectrometer systems affording $m/\Delta m_{50\%}$ resolution of over 400,000 it is still analytically challenging to
507 differentiate between isomeric components and often complex MS^n experiments are required to
508 achieve selectivity for unambiguous assignment. Ion mobility can provide extra resolving power,
509 however IMS used alone is currently unable to unambiguously identify an unknown molecular
510 component without *a priori* knowledge of the measured drift time.
511
512 It is possible to measure the resolving power of ion mobility using a single quotient definition (Siems
513 et al., 1994):

$$R = dt / \mathrm{w}h \qquad (6)$$

515
516 where R is the resolving power of the IMS, dt is the drift time of the ion of interest and $\mathrm{w}h$ is the full
517 peak width measured at half height. Resolving power is a measure of the efficiency of an instrument
518 to separate two peaks. The Waters Synapt G2 IMS system has been developed to encompass a
519 resolving power of up to 40; FAIMS resolving powers of up to 100 (Shvartsburg et al., 2010b) have
520 been achieved, and several reports of resolving powers of up to 225 with DT-IMS have been reported
521 (Koeniger et al., 2006; Shelimov et al., 1997; Kemper et al., 2009). Developments including higher
522 pressure trapping and focussing (Clowers et al., 2008), overtone ion-mobility (Valentine et al., 2009)
523 and circular instruments (Bohrer et al., 2008) are expected to exceed these current limitations.
524
525 The number of theoretical plates is a mathematical concept, relevant in any chromatographic
526 technique, which is often used to describe column efficiency and is an indirect measure of the peak
527 width for a peak at a specific retention time:
528

$$N = 5.545 \left(\frac{t_R}{W_h} \right)^2 \qquad (7)$$

530
531
532
533 where N = number of plates, t_R = retention time and W_h = peak width at half height (in units of time).
534 The number of theoretical plates is typically used to compare chromatographic systems and the data
535 in Table 2 compares various types of IMS with typical traditional chromatographic techniques.
536
537 **TABLE 2.** A comparison of required resolving power in theoretical plates for various types of IMS
538 compared to typical chromatographic conditions.
539

Approximate number of theoretical plates	Required resolving power of equivalent	Comparative chromatography conditions

	IMS	
20000	60	High performance liquid chromatography (HPLC)
80000	120	Ultra high performance liquid chromatography (UHPLC)
125000	150	Gas chromatography (GC)
222000	*200*	*High resolution IMS (Asbury & Hill, 2000a)*
887000	400	Capillary electrophoresis (CE)

540
541 Therefore, a current high-resolution IMS resolving power of 200 is roughly equivalent to a
542 chromatographic efficiency of >200,000 theoretical plates.
543
544 **Peak capacity of IMS-MS**
545 Complex samples require high efficiency to achieve separation and, even in early stage drug
546 discovery, having a high efficiency affords a good opportunity to separate degradants and process
547 impurities away from the desired product. Peak capacity is defined as the maximum number of peaks
548 that can fit in any two-dimensional method (Ruotolo et al., 2002a). A two-dimensional method will
549 have a high peak capacity if the resolution of each dimension is high and the difference in their
550 separation mechanism (orthogonality) is high. The peak capacity will also be defined by the
551 complexity of the sample and the properties of the analytes in the sample. For example, complex
552 biological samples with a range of retention times will provide larger peak capacities for a technique
553 than that of the analysis of a mixture of analytes of a specific class. Peak capacity is therefore a
554 better, but highly molecule dependent, indicator of the separation power compared to measuring
555 resolution alone.
556
557 In an ideal situation the peak capacity of a two-dimensional method is the product of the first and
558 second dimensions (Li et al., 2009), but corrections can be made for cases where the two dimensions
559 are not 100% orthogonal. Whilst the separation based on their size to charge ratio (Ω/z for IMS) and
560 mass to charge (m/z for MS) ratio is, to some extent, orthogonal there is a well-known correlation
561 between mobility ($\propto$ size) and mass (Griffin et al., 1973), as illustrated in Figure 12.
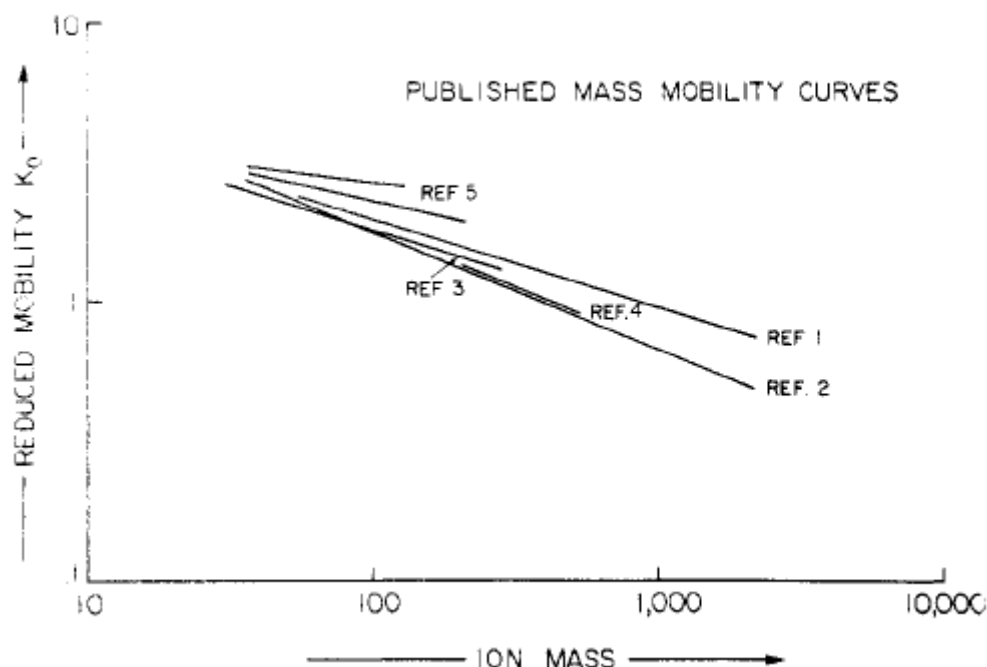
562
563 **FIGURE 12.** Published mass mobility curves showing correlation between reduced mobility and mass
564 within classes, but poor correlation in heterogeneous sets, adapted from Griffin et al. (1973).
565
566 Therefore the corrected peak capacity, **P_c**, in IMS-MS can theoretically be estimated (Dwivedi et al.,
567 2010) using the relationship:

$$P_c = R_{IMS} \times R_{MS} \times \text{fraction of orthogonality} \qquad (8)$$

where R_{IMS} is the average resolving power of the ion mobility spectrometer, and R_{MS} is the average resolution of the mass spectrometer.

An example of increased peak capacity in IMS-MS was observed in a study of various classes of metabolites in blood (Dwivedi et al., 2010) including amino acids, organic acids, fatty acids, purines etc) using a DT-IMS-MS system. In the mass range of 23 – 830 m/z, the drift time spread of ~14.3 ms results in ~28% of the total 2D space, or an average deviation in drift time of ±14% along the theoretical trend. With an average IMS resolving power of 90, average MS resolution of 1500, and ±14% orthogonality, the estimated peak capacity, P_c, for the instrument is 90 x 1500 x 14% = 18,900. The relatively low MS resolution of 1500 (peak width is 0.27 Da at an average mass value of 404 m/z) in this study (Dwivedi et al., 2010) resulted in an estimated peak capacity of MS alone of 2989. A six fold increase in the peak capacity was therefore observed (~19,000) in IMS-MS compared to MS alone (~3000).
Reverse phase chromatographic columns are routinely used to separate small molecules and the peak capacity for gradient elution high performance liquid chromatography was found to be typically up to 300 (Guo et al., 2009), and up to 400 (Wren, 2005) for gradient elution ultra-performance liquid chromatography. Comparing the peak capacity for different types of IMS with typical traditional chromatography peak capacities (Table 3) shows that the extra dimension of IMS is potentially a powerful separation tool.

TABLE 3. Approximate separation peak capacity for various analytical separation methods*.

Technique	Approximate peak capacity
FAIMS	*8.9 -44 (Canterbury et al., 2008)(Schneider et al., 2010b)*
DT-IMS	*90 (Dwivedi et al., 2010)*
HPLC	300 (Guo et al., 2009)
UHPLC	400 (Wren, 2005)
MS	3000 (Dwivedi et al., 2010)
IMS-MS	*19000 (Dwivedi et al., 2010)*
LC-MS	900000
LC-IMS-MS	*11340000 (Dwivedi et al., 2010)*

*Ion mobility and hyphenated techniques are italicized

It is conceivable that LC-IMS-MS may become a standard addition or replacement for LC-MS systems due to the ease of configuration and the increase in separating power. Indeed many proteomic applications are increasingly using LC-IMS-MS to separate complex peptide mixtures, leading to unprecedented extensive proteome maps (Liu et al., 2007b; Taraszka et al., 2005). LC-IMS-MS often does not require careful configuration, demanding sampling rates and does not appear to suffer from robustness issues compared to many two-dimensional techniques such as LCxLC, GCxGC etc.

Modifying selectivity in IMS
The selectivity of ion mobility can be modified by increasing the electric field in DT-IMS (Wu et al., 1998), the use of covalent shift reagents (Fenn and McLean, 2008) to derivatise or non-covalent shift reagents (Clowers and Hill, 2006; Howdle et al., 2009) to form complexes with analytes and effect a selective shift in ion mobility relative to coincident analytes, using drift gas modifiers (Fernández-Maestre et al., 2010a) sometimes called clustering agents in DMS-MS (Schneider et al., 2010b)), by altering the composition of the drift gas (Matz et al., 2002) and by the use of different reagent gases in GC-IMS-MS (Eiceman et al., 1995). Currently there does not appear to be a consensus on useful and well characterised selectivity modifiers so method development is presently not fully predictable; however some of these changes are trivial and can be considered analogous to changing the stationary or mobile phases in liquid chromatography.

The use of covalent shift reagents (Fenn and McLean, 2008), as shown in Figure 13 , effectively derivatises molecules, potentially creating lower density analogues of the precursor species with a marked increase in the collision cross-section relative to a smaller increase in mass. This is clearly

illustrated by deviations to larger cross sections compared to the general trend in mass-mobility correlation for carbohydrates. Compared to the underivatised species it was reported that covalent derivatisation afforded three distinct advantages: (i) tuneability was increased for isobaric species difficult to identify and/or resolve by mass spectrometry alone, (ii) an enhanced sensitivity of 2x more signal intensity was observed and (iii) the derivatised species could be used as tags or fragment labels in CID and as IR active species in IRMPD studies.
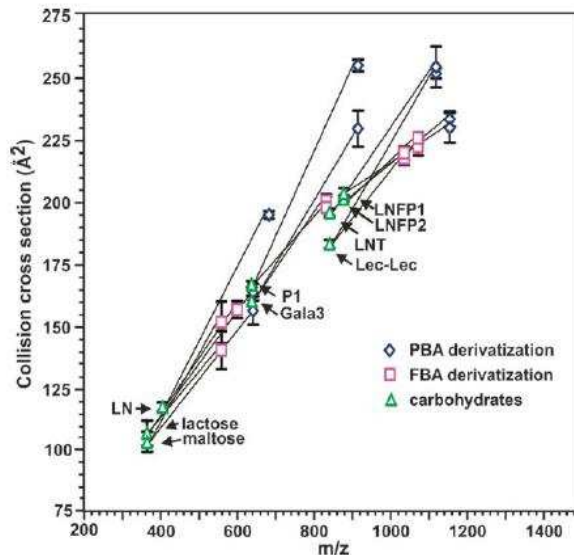
FIGURE 13. Effect of derivatisation of carbohydrate species with boronic acid on CCS, adapted from Fenn and McLean (2008).

For small molecules the effect of the dipole interaction is typically far more significant than for large molecules (>500 Da) so that using drift gas modifiers or mixtures can be a powerful method to alter selectivity (elution order of analytes). Indeed for small molecules such as amino acids the polarisabiity has been found to be a critical factor affecting separation of analytes, whereas in large molecules the collision cross section term dominates (Steiner et al., 2006). Thus for small molecules exploiting polarizability to probe structural details and maximize separation has immense future potential.

An example of the potential of exploiting polarizability to separate analytes is given by the different slopes of calculated ion radii for iodoaniline and chloroaniline with different drift gases, helium (0.205 x 10^{-24} cm^3), argon (1.641 x 10^{-24} cm^3) and carbon dioxide (2.911 x 10^{-24} cm^3), indicating that it should be possible to separate any analytes with different slopes (Figure 14) by choosing an appropriate drift gas composition.
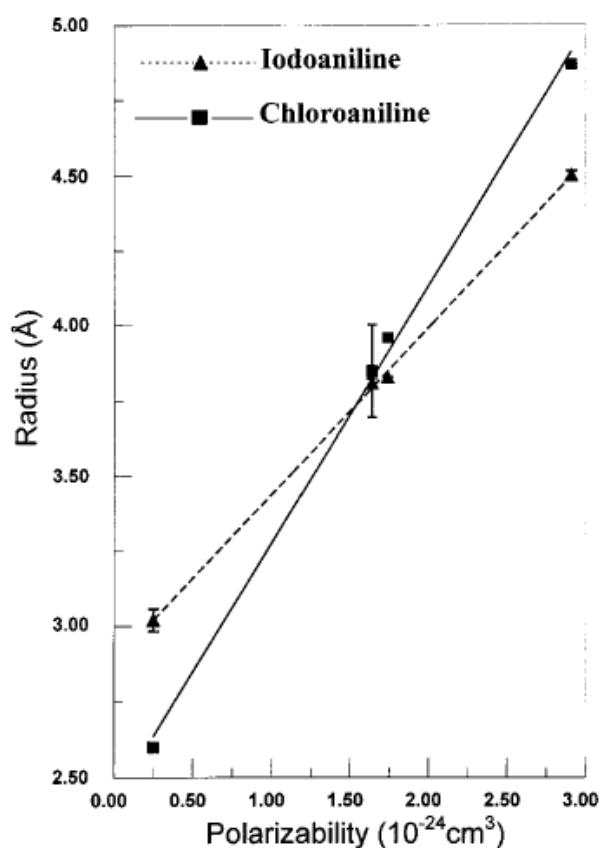
FIGURE 14. Calculated ion radii as a function of drift gas polarizability, from Asbury & Hill, 2000c.

The use of vapour modifiers added to the drift gas in planar DMS-MS has been widely explored (e.g. Levin et al., 2007 and Eiceman et al. 2004) , although the full mechanism of the interactions has not been elucidated enough to enable predictable separations in mixtures. Levin et al.   (2004) systematically examined the effect of various polar clustering agents and postulated strong effects due to hydrogen-bonding potential, electrostatic attraction, steric repulsion and energetically feasible conformations. A series of publications exploring the cluster/declustering (Krylov et al. 2002, Krylov et al. 2009, Schneider et al. 2010a, Schneider et al. 2010c, Coy et al. 2010) further explored the possibility of predicting analyte shifts in response to changes in drift gas modification and provide a powerful route to optimising separations.

The 'cluster/declustering effect' that addition of vapour modifier induces appears to have dramatic effects on the peak capacity in a planar electrode configuration (Schneider et al., 2010b), improving the peak capacity for a 70 component mixture from 13 in pure nitrogen to 44 in 2-propanol doped nitrogen (see FIGURE 15), although this had the disadvantage that 10/70 components were depleted in intensity by 20-fold or more due to them having a lower proton affinity than the dopant.
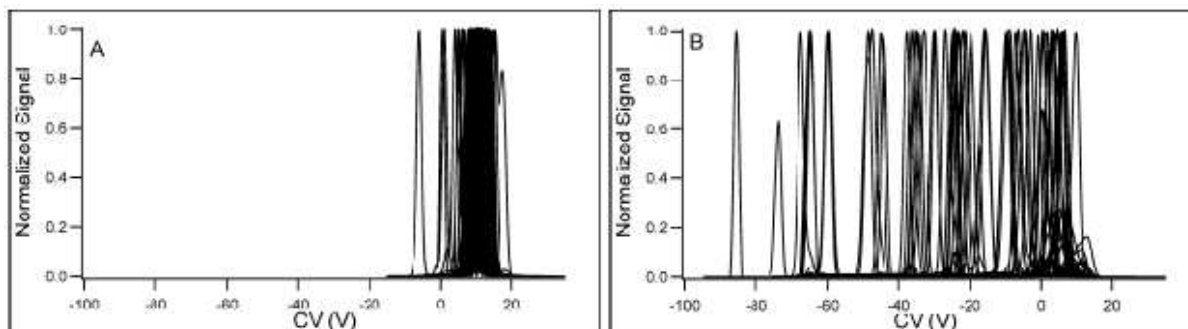
FIGURE 15. Separation of a 70-compound mixture with (A) nitrogen transport gas and (B) nitrogen with 1.5% 2-propanol in parallel plate FAIMS configuration, adapted from Schneider et al., (2010b).

Changes to the temperature, composition (Beegle et al., 2001) and pressure of a single drift gas is commonly used to change selectivity and IMS gasses including nitrogen, air, helium, carbon dioxide and sulphur hexafluoride have been evaluated. The use of binary gas mixtures (Howdle et al., 2010), shown in Figure 16, results in excellent selectivity enhancements over single gas composition IMS separations and demonstrates that this selectivity is tunable by altering the binary gas composition.
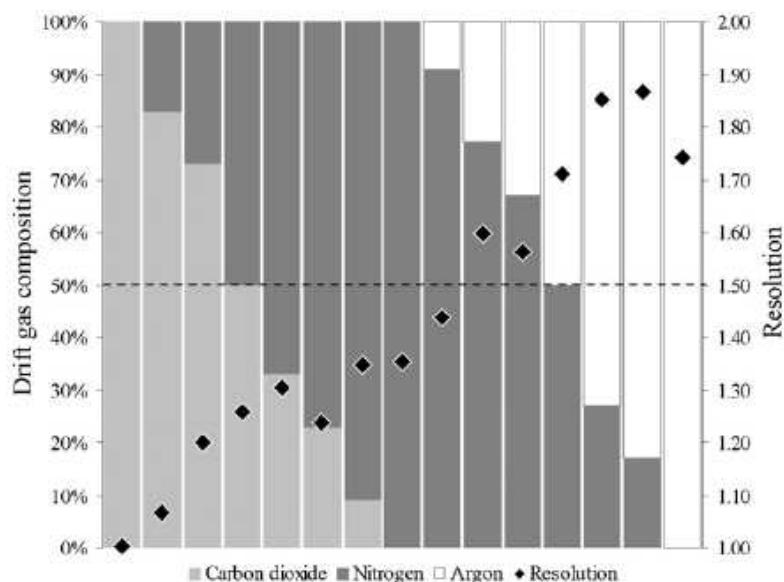
FIGURE 16. Effect of drift gas composition on the ion mobility resolution of the drugs rosiglitazone and lamotrigine [M+H]$^+$ ions in binary drift gas mixtures in TWIMS. The composition of the binary drift gas mixtures are represented by shaded bars indicating the percentage of each gas in the mixture (left hand axis). Resolving powers greater than 1.5 indicate full separation of components and this threshold is indicated by the dashed line at a resolution of 1.5. The resolution of lamotrigine and rosiglitazone is indicated by the right hand axis. Adapted from Howdle et al., (2010).

IV. APPLICATIONS OF IMS AND IMS-MS SEPARATIONS IN SMALL MOLECULE ANALYSIS

IMS has been investigated for the analysis of a wide range of small molecule applications including active pharmaceutical ingredients (Budimir et al., 2007; Karimi and Alizadeh, 2009; O'Donnell et al., 2008; Wang et al., 2007) veterinary drugs (Jafari et al., 2007), metabolites (Alonso et al., 2008), pesticides (Jafari, 2006; Keller et al., 2006; Tuovinen et al., 2000), prescription and illicit drugs (Dussy et al., 2008; Lawrence, 1986), combinatorial libraries (Collins and Lee, 2001), autonomous health diagnostics (Zhao et al., 2010) and immunoassay detection (Pris et al., 2009; Snyder et al., 1996). Here we outline some highlights of small molecule analysis using IMS-MS systems.

A. Low abundance metabolite and small molecule identification using IMS-MS

A novel use of LC-IMS-MS was demonstrated for a $5HT_3$ antagonist, ondansetron, and its aromatic hydroxyl isomeric metabolites (Dear et al., 2010) that are typically generated *in vivo* and *in vitro*. Using conventional UHPLC-MS-MS the unambiguous characterisation of the hydroxyl metabolites would not be possible as they can produce identical MS/MS spectra. Using UHPLC-MS in a biological matrix system ondansetron and metabolites display different retention times but could not be assigned without using purified standards as a reference. Using an IMS separation, shown in Figure 17, and *in silico* methods the components were identified based on their ion mobility. For these components a low number of rotatable bonds are present so the computational method is rapid, interpretation of complex NMR spectra is not required and isolation or synthesis is unnecessary to create primary standards. In this case the identity of metabolites with smaller than 1 $Å^2$ difference between their CCS was distinguished using a combination of Waters Synapt TWIMS by comparison with CCS values obtained using computational methods.
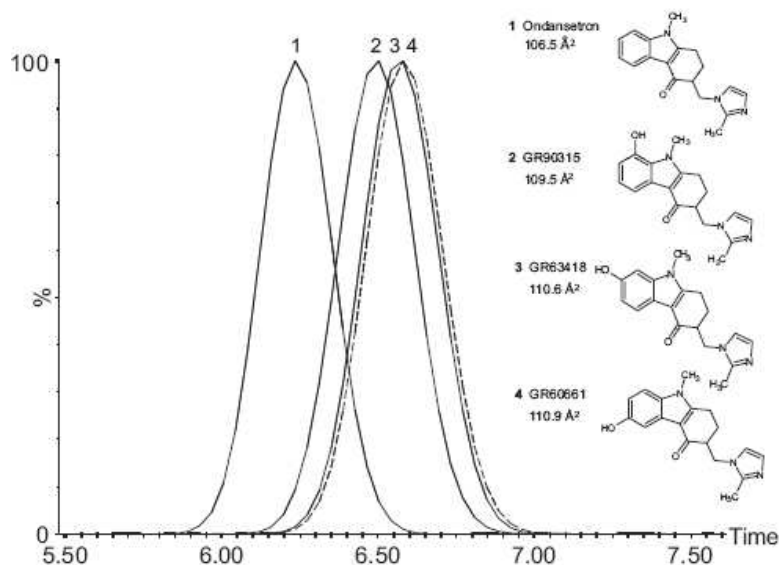

FIGURE 17. TWIMS ion mobility arrival time distributions for ondansetron and the 6-, 7- and 8-hydroxyl metabolites, adapted from Dear et al., (2010).

The subsequent use of product ion mobility as a tool for assignment of positional isomers (Cuyckens F et al., 2011) was also demonstrated for both model compounds and a real-case example, emphasizing the possibilities of structural determination by both parent ion and product ion mobility where mass spectra alone appear indistinguishable and cannot be used to confidently assign a candidate structure. For example two different product ion mobilities for 11 *ortho*, *meta* and *para* substituted hydroxyl metabolites with a phenylethylamine substructure were sufficient to assign their structures.

B. Rapid, portable and sensitive analysis using miniaturisation of IMS and IMS-MS

One of the advantages of FAIMS is that it does not require complicated vacuum equipment or large analyser tubes, thus it may be easily hyphenated to a portable mass spectrometer system (Manard et al., 2010). Microfabricated FAIMS chips can increase the speed of separation by 100-10,000 times, filtering ions on the microsecond timescale enabling rapid monitoring of species at low level concentrations (Shvartsburg et al., 2009a). Whilst the current microfabricated FAIMS units, example shown in Figure 18, are more suited to distinguish compound classes than individual species the multichannel FAIMS electrodes enables integration with an air sampler, ionisation source and detector for applications such as gas analysis, chemical monitoring and autonomous health diagnostics (Zhao et al., 2010).
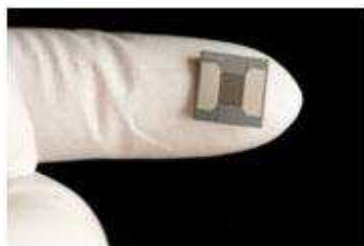
720

721 **FIGURE 18.** Illustration of the size of microfabricated FAIMS chip, courtesy of Owlstone
722 Nanotechnologies and Pacific Northwest National Laboratory.

C. Increased selectivity in ambient and surface analysis mass spectrometry using IMS-MS

724 The direct and rapid analysis of substances using ambient ionisation mass spectrometry sources
725 allows mass spectrometry data to be obtained with little or no sample preparation required for a
726 variety of surfaces and matrices from tissue samples to intact tablet or liquid formulations. Application
727 areas have included quantitative and qualitative measurements in pharmaceutical analysis, forensics,
728 bioanalysis, *in vivo* imaging, proteomics etc. Whilst MALDI has been widely adopted in biological
729 applications, for the analyses of biomolecules, there is currently a great deal of interest in ambient
730 mass spectrometry approaches and there are now at least thirty methods documented (Weston,
731 2010).

733 The introduction of an additional IMS stage adds a further separation step to ambient mass
734 spectrometry analysis without the need for rigorous sample preparation. Indeed for most surface
735 analysis mass spectrometry methods the fact that the surface is sampled and ions are generated in a
736 single step means that the only viable method of separation and selectivity before the mass detector
737 is to use a gas-phase separation method such as IMS. This extra selectivity maybe particularly useful
738 in imaging applications. In the case of the example of whole-body imaging of rats, the rats were dosed
739 with 6 mg/kg *iv* with the anticancer drug vinblastine and the removal of interfering isobaric ions from
740 endogenous lipids helps increase confidence in the MALDI imaging data (Jackson et al., 2007) by
741 removing 'false positives' which, by mass spectrometry imaging alone, could be interpreted as
742 containing a high concentration of the active drug, as shown in Figure 19. The extra dimension of
743 separation could also prove useful in removing any matrix-related isobaric ions. The datasets from the
744 Driftscope imaging platform were transferred to Biomap 3.7.5.5 for visualization enabling facile
745 interpretation.
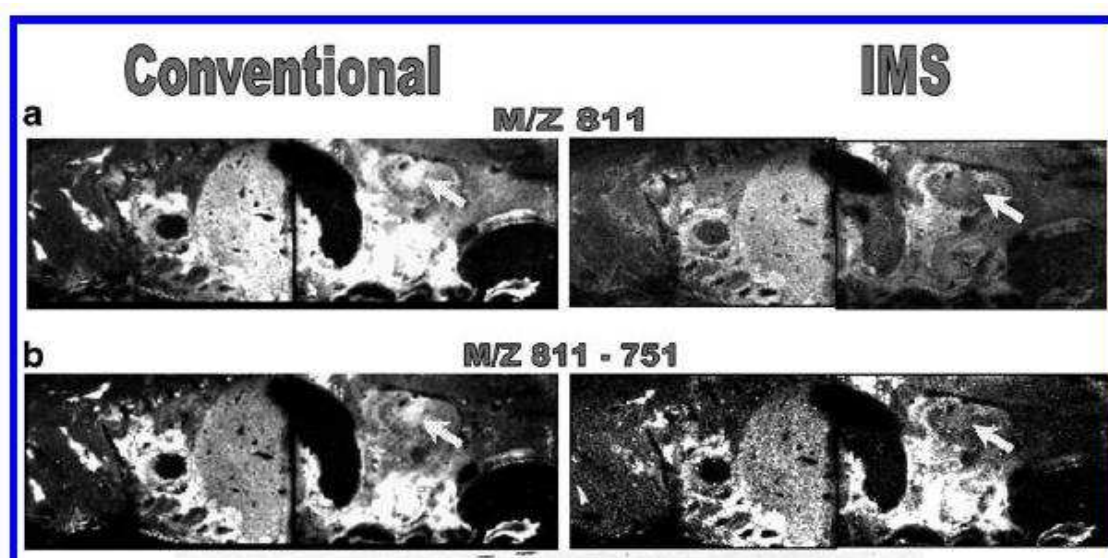
746
747 **FIGURE 19** . MALDI-IMS-MS image showing distribution of ions in whole-body sections and the
748 arrow points to the area where specificity increased with application of IMS, adapted from Jackson et
749 al., (2007).
750

751 **D. Chiral analysis using IMS-MS**
752 A chiral modifier at 10 ppm of (S)-(+)-2-butanol was added to the buffer gas and enantiomers of a
753 β-blocker, atenolol, were separated (Dwivedi et al., 2006), as shown in Figure 20. It is proposed that
754 selective interactions occur in the gas-phase between the enantiomer ion and the chiral modifier, to
755 temporarily form a diastereomeric pair, so that the mobilities of the enantiomers are altered and can
756 be separated in time. Chiral ESI-DT-IMS-MS is now commercialised viathe Excellims Corp IMS-
757 quadrupole-MS system. A smaller, portable chiral IMS detector is now being developed by Excellims
758 Corp for fast, on-site analysis including pesticide residues and environmental samples (Anon). The
759 advantages of chiral IMS-MS compared to competing analytical techniques such as chiral SFC and
760 chiral HPLC include rapid method development and high sensitivity, enabling rapid determination of
761 enantiomeric excess (e.e.) for use in QA/QC environments or in broader applications including
762 biomarker and metabolite identification.
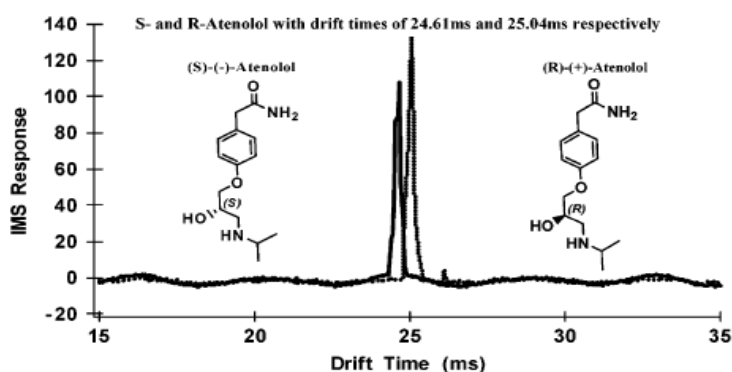
763
764

765 **FIGURE 20.** DT-IMS-MS separation of atenolol enantiomers showing the superimposed spectrum of
766 the R and S enantiomers (similar results obtained using racemic mixture, not shown). Adapted from
767 Dwivedi et al., (2006).

768 Chiral resolution using FAIMS-MS has also been reported for 6 pairs of amino acid enantiomers
769 separated as metal-bound complexes of divalent metal ion with an L-form amino acid (Mie et al.,

770 2007), shown in Figure 21. The method employed a range of additional divalent metal cations and
771 reference amino acids. Screening with different metal cations and reference compounds compares
772 favourably with chiral HPLC and SFC screening times and can be automated using automated
773 sample preparation platforms.

774
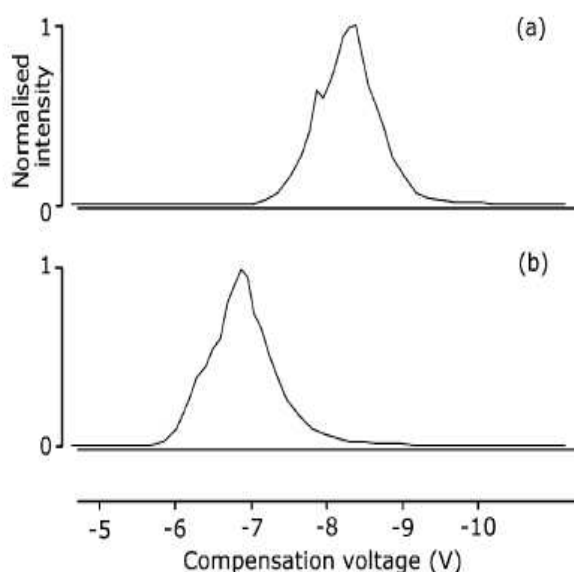
775 **FIGURE 21.** Separation of D/L-valine as $[Cu^{2+}(l-Trp)_2(D/L-Val)-H]^+$. (a) D-Val; (b) L-Val. Adapted from
776 Mie et al., (2007) .

777 An example of epimer separation where the diastereomers differ by only one chiral carbon, was
778 achieved for betamethasone and dexamethasone (Campuzano et al., 2011). The separation of the
779 two epimers correlated well with differences observed in the calculated B3LYP/6-31G++(d,p)
780 electrostatic potential surface. Whilst baseline separation is achievable by HPLC (Arthur et al., 2004)
781 the mass spectra of these compounds is very similar so the rapid separation and correlation with
782 molecular modeling quickly identify this pair of compounds.

783 **E. Resolution of isobars and isomers in complex mixtures using IMS-MS**

784 Over 1100 metabolites were detected from methanolic extracts of 50 ul of blood samples including
785 separation of over 300 isobaric/isomeric components, achieved without pre-concentration (Dwivedi et
786 al., 2010), shown in Figure 22. The peak capacity compared tomass spectrometric analysis alone was
787 increased by ~6 times and a broad range of metabolites were detected including lipids, carbohydrates,
788 isoprenoids and estrogens. Interpretation of the data is further enabled by examining characteristic
789 mobility-mass correlation data to identify similar classes of metabolites. In addition a reduction in the
790 background noise due to selective ion filtering enabled detection and identification of low abundance
791 components.
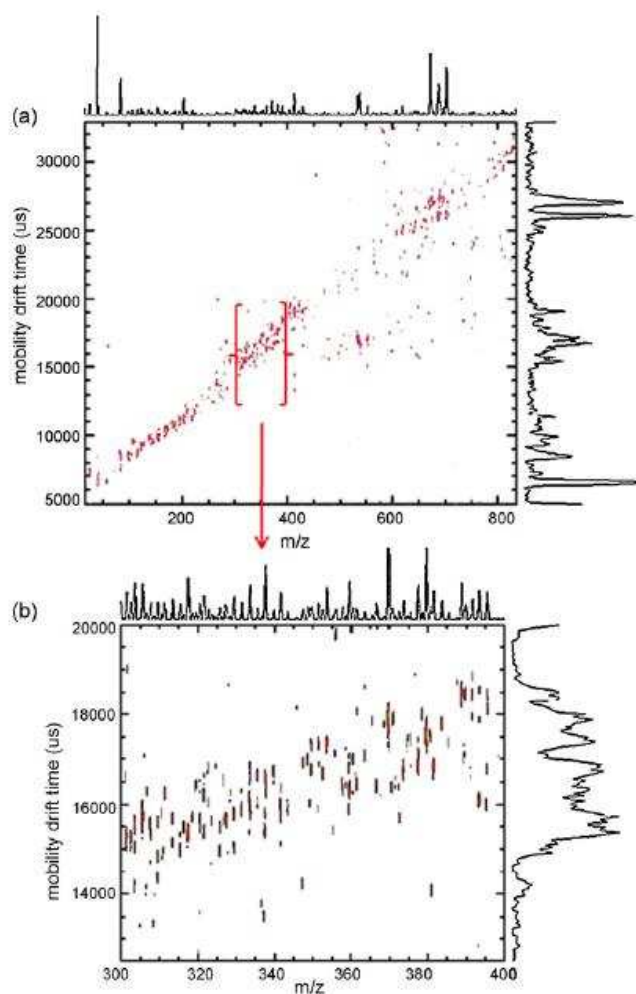
FIGURE 22. (a) Two-dimensional spectra of metabolic features measured in methanolic extract of human blood (b) a zoomed in region of the DT-IMS-MS spectrum illustrating peaks detected at the same nominal mass with different mobilities showing separation of isomers and isobars, adapted from Dwivedi et al., (2010).

F. Real-time reaction monitoring and process monitoring using IMS-MS

Reaction-monitoring in real-time has the potential to enable understanding of when reactions can be terminated at a suitable, rather than arbitrary, endpoint. By monitoring a process regularly throughout the reaction time knowledge may also be accrued of the reaction, intermediates and product formation that could not be understood by irregular, sparse sampling alone and enable optimization of experimental parameters via chemometrics. The products formed by deprotonation of 7-fluoro-6-hydroxy-2-methylindole with sodium hydroxide were monitored by TWIMS-MS (Harry et al., 2011) and showed complementary and extra information from TWIMS-MS compared to MS alone with shape selectivity information obtained by sampling every several minutes over a timescale of several hours (Figure 23).
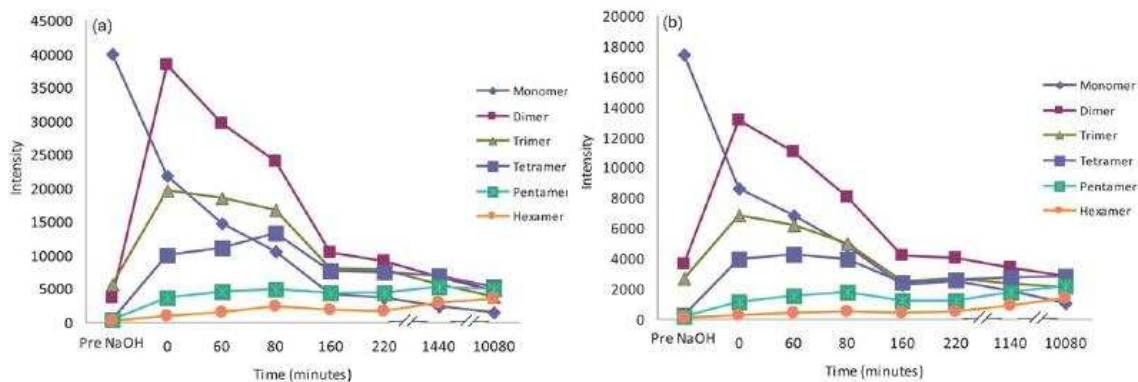
809

810 **FIGURE 23.** MS and TWIMS-MS analysis of the reaction of 7-fluoro-6-hydroxy-2-methylindole
811 following the addition of aqueous sodium hydroxide. Signal response versus time in minutes for m/z
812 166 (monomer, I), m/z 311 (*O*-linked dimer, II), m/z 456 (*O*-linked trimer), m/z 601 (*O*-linked tetramer),
813 m/z 746 (*O*-linked pentamer) and m/z 891 (*O*-linked hexamer) using (a) MS and (b) IM-MS. Adapted
814 from Harry et al., (2011).

815 **G. Rapid resolution of carbohydrate isomers using IMS-MS**

816 Carbohydrate isomers including oligosaccharides are involved in numerous biological processes,
817 such as cell-cell recognition and the development of embryos, but one of the main functions of
818 carbohydrates is as oxidisable substrates in catabolism. However, to fully understand their different
819 roles and functions we need to understand both the linkage type and anomeric configuration whilst
820 dealing with the challenge that, for example, in a mixture of 16 D and L-aldohexoses and 8 D and L-
821 aldoses the total number of isomers with the same mass will be 96. The use of mass spectrometry as
822 a tool is hindered by the similarity between fragmentation data obtained for different isomers; however
823 purification and determination of purity by NMR requires interpretation time and larger amounts of
824 material. Separation of the metal ion adducts of anomeric methyl glycoside isomers (MeMan, MeGal
825 and MeGlc) and isomeric forms of reducing sugars (Dwivedi et al., 2007), branch isomers, and very
826 closely related isomers varying at a single stereochemical position (Zhu et al., 2009) were addressed
827 where MS^n was not able to deliver solutions to the problem, as shown in Figure 24.
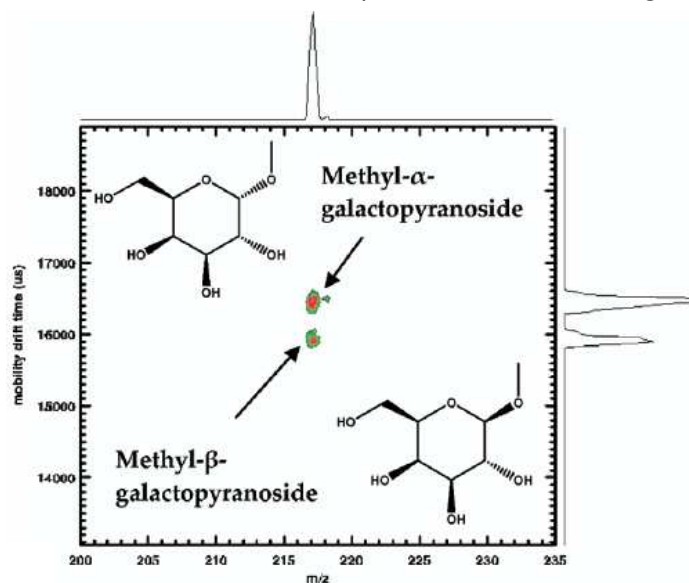
828

829 **FIGURE 24.** Two-dimensional DT-IMS-MS spectra of a mixture of methyl-α and β-D-
830 galactopyranosides showing the separation (N$_2$ drift gas) of the sodium adducts at m/z 217, adapted
831 from Dwivedi et al. (2007).

832

H. Rapid analyte testing in complex drug formulations by IMS-MS

The combination of IMS-MS with ambient ionisation mass spectrometry may enable rapid analysis for complex mixtures including drug formulations without laborious method development and consumables required by other separation methods such as 2D LC-MS etc.

The complementary techniques of IMS and DART ambient ionisation operated separately has been demonstrated for AG-013736 in 1 mg Axitinib tablets (Likar et al., 2011), enabling a rapid analysis of AG-013736 in AG-013736 drug substances by DART ionisation and analysis of low-level limits for absence of the drug in placebo tablets by ion mobility spectrometry using a Model 400B IONSCAN-LS from Smiths Detection Scientific (Danbury, CT).

Hyphenated ambient ionisation IMS-MS and nano-electrospray has been used to analyse:
- pharmaceutical formulations including tablets and creams containing one or more of ranitidine, paracetamol, codeine, anastrozole chlorhexidine and a nicotine-containing skin patch (Weston et al., 2005) using DESI.
- pharmaceutical formulations from tablets containing one or more of timolol, paroxetine, paracetamol and codeine using nano-electrospray ionisation (Budimir et al., 2007).
- pharmaceutical formulations containing one or more of paracetomol, ephedrine, codeine and caffeine from non-bonded reversed-phase thin layer chromatography (RP-TLC) plates by desorption electrospray ionisation (DESI) (Harry et al., 2009).

These examples demonstrate the wide applicability of analyses in various types of formulation illustrating that pre-treatment of samples is not required, rapid analyses can be conducted, whilst maintaining reproducible and robust results.

I. Analysis of supramolecular complexes using IMS-MS

The syntheses of supramolecular complexes that possess photo-optical properties are desired for solar energy capture and conversion, molecular machines, photochemical drugs and fluorescent-based sensors.
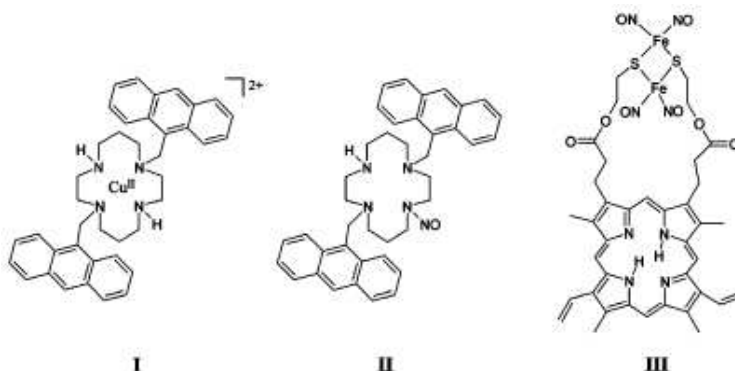
FIGURE 25. Schematic of $Cu^{2+}(DAC)^{2+}$ (**I**), DAC-NO (**II**), and PPIX-RSE (**III**), adapted from Baker et al., (2005).

DT-IMS-MS was used to probe the structures of bichromic complexes (Figure 25; Baker et al., 2005) in order to provide relevant data for sampling from *in situ* fluid data. Complementary data to ^{1}H-NMR, x-ray crystallography and fluorescence measurements were obtained.

For **I** the crystal structure agreed well with DFT structures and IMS-MS measurements, indicating that solid-state structures agreed well with gas-phase measurements. Only a single peak was observed in the ion mobilogram and calculation gave 161 $Å^2$ as the CCS, compared to 166 $Å^2 \pm 5$ $Å^2$ predicted from the DFT structure.

For **II** DT-IMS-MS measurements indicated two conformers by observation of two main bands in the ion mobilogram, by comparison with computational data this suggested two major families of Up-Up and Up-Down configuration, as shown in FIGURE 6. The solution NMR data for **II** also suggested two conformers but the structures could not be unambiguously determined from the data.
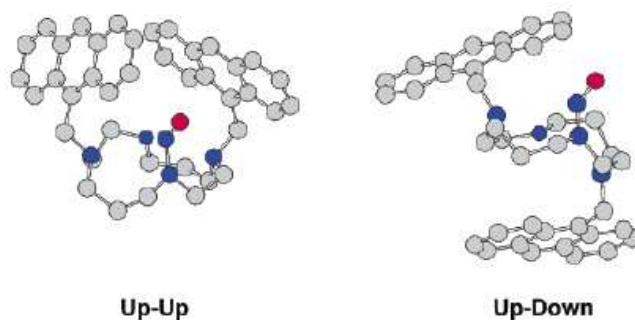
Up-Up   Up-Down

FIGURE 26. Examples of the two families predicted for (**II** + H)$^+$. The Up-Down family is the lower energy family, the Up-Up family has both anthracenyl groups on the same side as the cyclam. Adapted from Baker et al., (2005).

For **III** DT-IMS-MS measurements indicated two conformers which, in combination with DFT measurements indicated two compact structures, rather than folded structures, and correlated well with photophysical features including a bimodal fluorescent decay and a residual emission in steady-state luminescence experiments. The proportion of the two conformers measured by IMS-MS, shown in Figure 27, agreed well with pre-exponential factors that indicated an approximate 80:20 ratio.

FIGURE 57. ATD for (**III** + H)$^+$ obtained at 80 K. Two distinct peaks indicate two conformers of (**III** + H)$^+$ are present, adapted from Baker et al., (2005).

J. Hydration and desolvation of ligands and substrates

In drug design it is important to consider water molecules particularly in two situations:

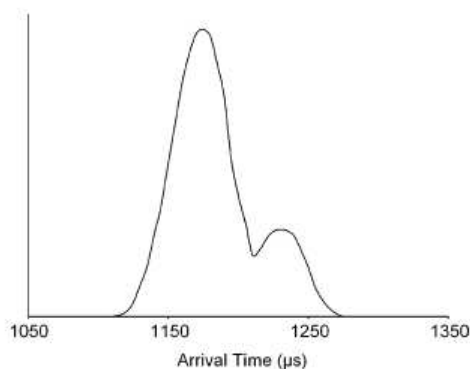   (i)   those water molecules that will be displaced during ligand binding in a receptor (Poornima and Dean, 1995), and

    (ii)   those water molecules that will be desolvated crossing the membrane environment.

Water in binding pockets in a receptor can provide surprising entropic and enthalpic contributions to structure and binding affinities (Pace et al., 2004; Homans, 2007). If the key water binding sites and influence of 'small molecule' ligands are known it may be possible to use this information in medicinal drug design, or to predict static hydration sites. It may be especially important to consider bridging waters that link ligand to protein via an extended hydrogen bond network.

Understanding membrane permeability is key to drug delivery and activity and is typically understood by hydrogen bond descriptors such as polar surface area (PSA) and surrogate measurements such as logD. These are considered important physicochemical parameters and modulated during lead optimisation. The reason that these parameters are important is that it is polar groups that are most involved in desolvation when molecules move from an aqueous extracellular environment to the lipophilic membrane environment. During this migration molecules may change their conformation and lose water molecules in order to cross the membrane barrier. To further understand the effect of desolvation on ligands it is possible to add/remove water molecules one by one by changing the water vapour pressure of the DT-IMS-MS cell and gradually ascertain the ion mobility and conformation adopted from a hydrated towards a non-hydrated ion, shown in Figure 28(a). By measuring the energy change at different temperatures a van't Hoff plot can be generated, shown in Figure 28(b), thereby revealing the entropic and enthalpic contributions to hydration.

(a)   **(b)**
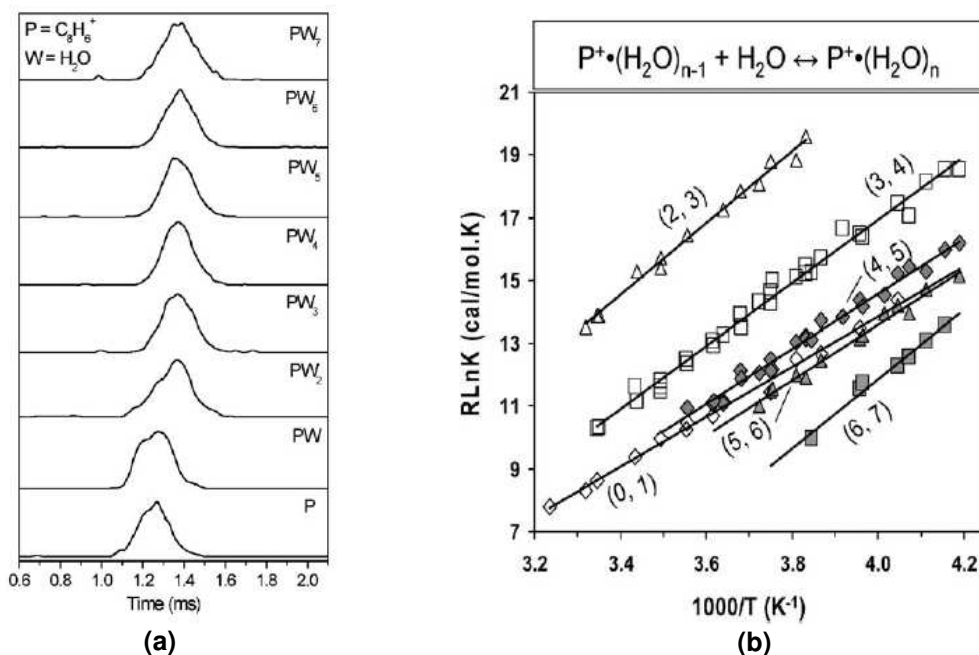
FIGURE 28. (a) ATDs of hydrated phenyl acetylene ions (PW$_n$) obtained following the injection of the phenyl acetylene ion (C$_8$H$_6$•+) into 0.34 Torr of water vapor at 249 K (b) Van't Hoff plots for the equilbria C$_8$H$_6$•+(H$_2$O)n-1 + H$_2$O $\Leftrightarrow$ C$_8$H$_6$•+(H$_2$O)n for n-1 and n as indicated. Adapted from Momoh & El-Shall., (2008).

Hydration of small molecules has been studied for the phenyl acetylene ion, with stepwise hydration energies of 39.7 ± 6.3 kJ mol^{-1} from n=1 to 7; the entropy change for step 7 is larger, indicating a cyclic or cage like water structure (Momoh & El-Shall, 2008). For the benzene ion stepwise hydration energies were 35.6 kJ mol^{-1} from n=1 to 6. The binding energies were larger in the n=7 and 8 clusters indicating cyclic or cage like water structures (Ibrahim et al., 2005). For small protonated peptides the hydration energy is largest for highly charged peptides and small non-arginine containing peptide and typically 30 to 60 kJ mol^{-1} (Wyttenbach et al., 2003); for pentapeptides AARAA, AARAA-OMe and Ac-AARAA the binding energies were typically ~41 kJ mol^{-1}.

The foregoing IMS-MS studies indicate hydration/desolvation studies of small molecule ions can provide structural information in the gas phase, this may be relevant to:
1) understanding water and hydrogen bonded networks (including their entropic consequences) involving protein, ligand and water as part of molecular recognition systems,
2) ligand desolvation on transport through membrane environments, and
3) hydrogen/deuterium exchange experiments and how they are effected by molecular conformation.

Other methods to measure the hydration of small drug-like molecules include infra-red data recorded from a hydrated electrospray source or a droplet ion source (Poully et al., 2008) but these have not always provided unambiguous data, possibly due to the lack of energy required for proton transfer. The measurement of hydration/desolvation energies, described above, may provide a unique insight into the energy landscape of hydration/desolvation by conducting measurements over a range of temperatures.

V. OVERVIEW OF COLLISION CROSS-SECTION (CCS) MEASUREMENTS FOR SMALL MOLECULES

In DT-IMS-MS and TWIMS-MS, larger ions (with a larger CCS) tend to migrate slower through the gaseous medium in the IMS cell compared to smaller ions due to a higher number of collisions with the gas molecules (typically an inert gas such as nitrogen). The drift times through the IMS cell can also reveal structural information such as size, shape and topology; potentially including information

945   relating to accessible conformations. Unfortunately DMS and FAIMS are, currently, not suitable for
946   carrying out CCS measurements.
947
948   Understanding small molecule structure in the gas-phase may be advantageous for quality control or
949   for a more detailed understanding of molecular structure in the gas-phase. For example in drug
950   discovery the physicochemical and binding properties of small molecules depend on their 3D
951   structure and at physiologically relevant temperatures a conformationally flexible small molecule is
952   expected to be able to access a number of energetically feasible conformers, an example is shown in
953   Figure 29. The timescale of interconversion of conformers will define the structural information that
954   can be obtained in solution and in the gas-phase. Understanding the energetics of small molecule
955   conformers is currently largely carried out by generating potential conformers, known as
956   conformational sampling, in computational studies (Foloppe & Chen, 2009).
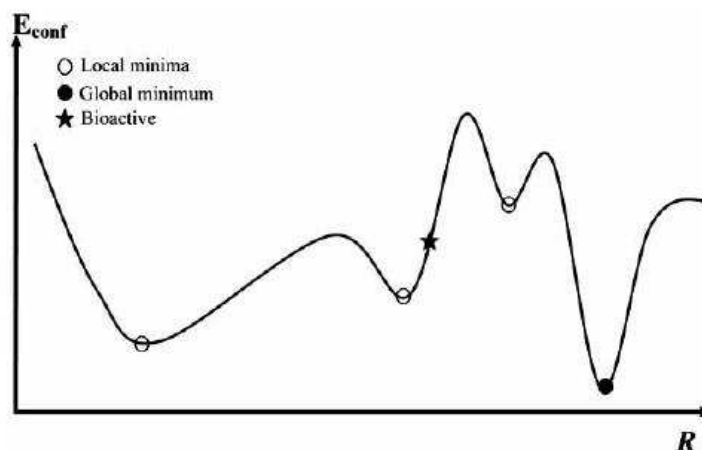
957

958   **FIGURE 29.** Hypothetical example of a one-dimensional molecular conformational potential energy
959   surface. Conformational degrees of freedom (R) are shown on the X axis. Adapted from Foloppe &
960   Chen (2009).

961
962   Computationally sampled models have been compared with x-ray crystallographic structures to
963   understand how well the conformer models correlate with the bioactive conformation. Solution NMR
964   can provide valuable information about the 3D structure; however the interpretation is often difficult
965   due to the exchange between several conformations and typically requires molecular modelling to
966   interpret results.
967
968   Rapid calculation of CCS by IMS-MS may be useful to decide which molecules in a library (series)
969   could provide the optimum activity. This could be achieved coarsely by excluding molecules which are
970   too rigid/flexible or too big/small as suggested by Williams et al. (2009a). These experiments
971   potentially have the advantage of rapid speed of experiment and low consumption of sample relative
972   to NMR and x-ray techniques. Understanding the conformation in the gas-phase may be a good
973   indicator of the bioactive conformation. This may be especially relevant to compounds in drug
974   discovery which are challenging to isolate and characterise their structure. Mapping the
975   conformational landscape defined via stereo-centres, intramolecular cyclisation etc., may help
976   uncover a path to identification of new target compounds.
977
978   For protein structures there is now significant evidence that the gas-phase protein structure can
979   reflect the native state solution phase structure under certain carefully controlled conditions. There
980   have been several publications that demonstrate a good correlation between x-ray, NMR and IMS
981   studies for protein structures (Heck and van den Heuvel, 2004; Rand et al., 2009; Ruotolo et al., 2005;
982   Schultz and Solomon, 1961; Shelimov et al., 1997; Shelimov and Jarrold, 1997), although there have
983   also been some differences noted (Jurneczko and Barran, 2011). However for small molecular
984   weight molecules the evidence that gas-phase structures are similar to solution phase structures has
985   been questioned; in a protein there are multiple cooperative interactions that maintain the 3D
986   structure whereas for a small molecule there are typically fewer interactions resulting in a more
987   flexible structure. Furthermore Allen et al. (1996) compared a range of gas-phase and x-ray molecular
988   substructures for small molecules and suggested that high-energy conformers were represented more
989   in gas-phase, room-temperature Boltzmann distributions than in crystal structures and broad peaks

990   observed in IMS have generally been interpreted as indicating that multiple conformations are
991   accessible and interconvert on the IMS measurement timescale.
992

993   Measurements using IMS-MS may not be the same as NMR (which are subject to solvent effects) or
994   x-ray (which are subject to crystal lattice effects). In enzymes and membrane receptors, biomolecular
995   recognition processes are likely to take place in hydrophobic 'binding pockets' of proteins where there
996   will then be several interactions for a ligand including hydrophobic amino acids, with a large possibility
997   (>0.8) of excluding most water molecules. The dielectric constant of a partial vacuum in IMS-MS (c.f.
998   ε_{vacuum} = 1) is more similar to the immediate environment of a membrane receptor ($\varepsilon_{peptide/protein}$ = 2–4)
999   than for water (ε_{water} = 80)(Bastug and Kuyucak, 2003). We may therefore postulate that the
1000   environment of a bioactive conformer will often be intermediate between aqueous and gas-phase
1001   (vacuum). Therefore the gas phase may be an appropriate medium in which to study the 'small
1002   molecule' structures which in their active form are bound to a receptor located in a membrane, rather
1003   than in solution.

A. CASE STUDIES OF COLLISION CROSS-SECTION (CCS) MEASUREMENTS FOR SMALL MOLECULES

1. Study of an organoruthenium complex and its adducts with a DNA oligonucelotide

1007   TWIMS-MS has been used to understand the binding of a "piano-stool" shaped organoruthenium
1008   complex with a single stranded oligonucleotide hexamer that show promise as an anti-cancer agent.
1009   The illustration in Figure 30 shows examples of the protonated and deprotonated complexes, the
1010   doubly positive charged complex and the doubly negative charged complex. The single peak (A)
1011   suggests a single species, whereas multiple peaks in (B), (C) and (D) suggest either multiple binding
1012   of the Ru-drug fragment (confirmed by interpretation of the mass spectra collected) or different
1013   conformers present in the mononucleotide due to different charge distributions along the phosphate
1014   backbone (Williams et al., 2009a).
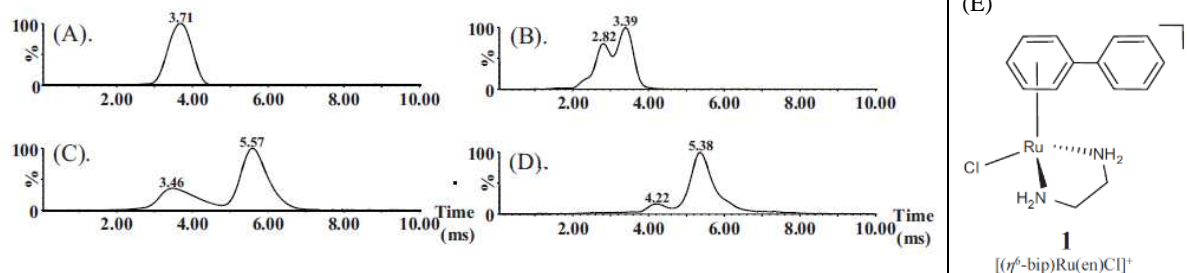
FIGURE 30. Arrival time distributions (ATDs) or drift times for (A) the $[M+2H]^{2+}$ ion of d(CACGTG); (B) the $[M-2H]^{2-}$ ion of d(CACGTG); (C) the complex $[CACGTG+2[(\eta^6\text{-bip})Ru(en)]-2H]^{2+}$; and (D) the complex $[CACGTG+2[(\eta6\text{-bip})Ru(en)]-6H]^{2-}$ and (E) structure of the organoruthenium anticancer complex $([(\eta^6\text{-bip})Ru(en)])$, adapted from Williams et al., (2009a).

1021   The CCS values obtained for the Ru-based drug correlated well with those obtained by x-ray
1022   crystallographic data so that binding could be easily identified. Using MS/MS experiments, shown in
1023   Figure 31, subsequent to IMS separation, enabled the binding site to be determined by examining the
1024   resulting fragmentation pattern.
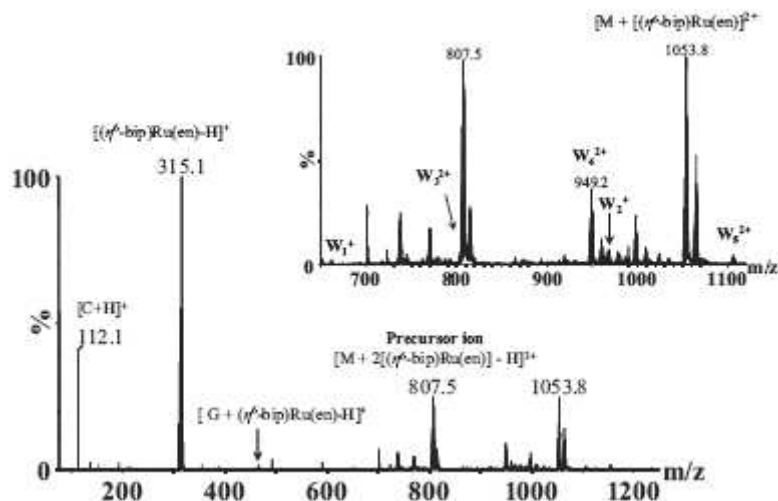
1025

FIGURE 31. MS/MS spectrum of the precursor ion of m/z 807.5, corresponding to [CACGTG+2[(η6-bip)Ru(en)] H]$^{3+.}$ Inset shows the relevant sequence-specific ions detected. (Note: M represents CACGTG), adapted from Williams et al., (2009a).

2. Study of the in-flight epimerisation of a bis-Tröger base

The epimerisation pathway via the proposed alternatives of a) a proton catalysed ring opening or b) retro-Diels-Alder of a bis-Tröger base, shown in Figure 32, were investigated using TWIMS-MS (Révész et al., 2011) as this could be important for the design of Tröger bases which, with their tweezer type structure, have been suggested as useful agents as molecular receptors, chiral solvating agents and inclusion complexes (Maitra et al., 1995).
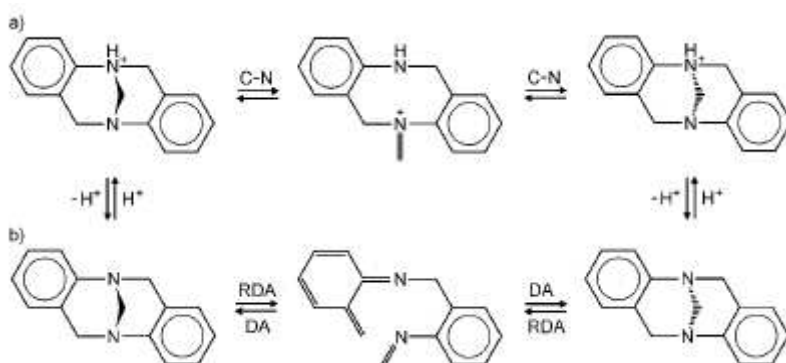
FIGURE 32. Proposed mechanism for epimerisation of a Tröger base by a) a proton catalysed ring opening or b) a retro-Diels-Alder mechanism, Révész et al., (2011).

The two structures were separated well in the gas-phase TWIMS stage (FIGURE 33) and activation of ions pre-TWIMS separation and post-TWIMS separation demonstrated that the anti-1H$^+$ isomer is the most thermodynamically favoured by measuring the intensity of each parent ion. The preferred mechanism was also concluded to be the proton catalysed ring opening as demonstrated by the lack of epimerisation when a Na$^+$ Tröger base was used as a surrogate proton-like participant in the reaction, thus eliminating the possibility of a retro-Diels-Alder mechanism.
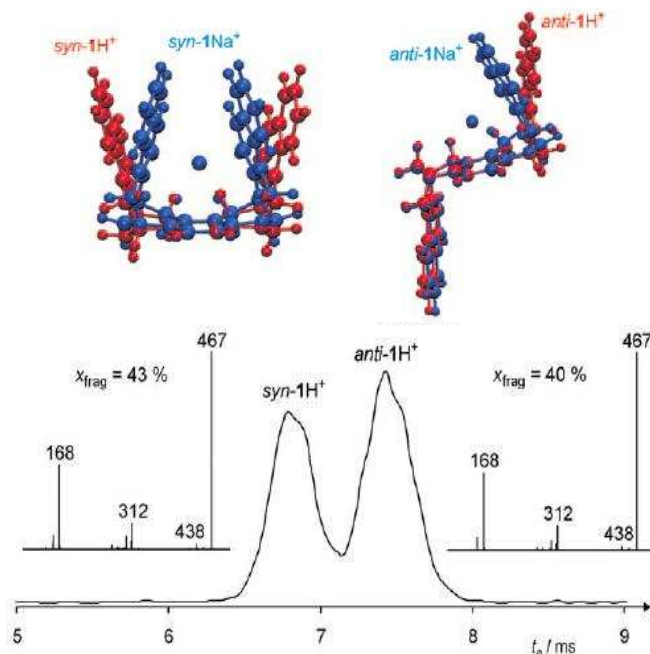
FIGURE 33. Ion mobility trace with associated mass spectra (shown inset) of the *anti-* and *syn-* isomers. The computationally calculated structures are shown above, adapted from Révész et al., (2011).

B. Measurement of collision cross-section (CCS) for small molecules using DT-IMS-MS

The measurement of CCS in DT-IMS is simplified by the use of a static, uniform, electric field in which ion motion takes place; the physical principles are established and mobility values can be used to derive the collision cross-section. Knowing the length of the drift region and the time that ions take to traverse it enables the ion's velocity to be determined:

$$v = \text{KE} \rightarrow \frac{\text{L}}{\text{t}_\text{d}} = \text{K}\frac{\text{V}}{\text{L}} \rightarrow \text{K} = \frac{\text{L}^2}{\text{Vt}_\text{d}} \tag{9}$$

where v is the ion's velocity, K is the ion mobility constant, E is the electric field, L is the length of the drift tube, t_d is the arrival time and V is the voltage across the drift region.

K should be corrected for temperature and pressure to obtain the reduced ion mobility, K_0 (corrected to 273 K and 760 Torr):

$$\text{K}_0 = \text{K}\left[\frac{273}{\text{T}}\right]\left[\frac{\text{P}}{760}\right] \tag{10}$$

The collision cross-section, Ω_T, can then be derived directly:

$$\Omega_\text{T} = \left(\frac{3\text{ze}}{16\text{N}}\right)\left(\frac{2\pi}{\mu k\text{T}}\right)^{1/2}\left(\frac{1}{\text{K}}\right) \tag{11}$$

where Ω is the collision cross-section, ze is the ionic charge, N is the background gas number density, μ is the reduced mass of the ion-neutral pair, k is Boltzmann's constant, T is the gas temperature and

1078 K is the mobility constant.

1079 **C. Calculation of collision cross-section (CCS) for small molecules using TWIMS**
1080 The measurement of CCS in TWIMS is not typically directly derived from the mobility of an ion (Giles
1081 et al., 2010) as the motion of the analyte in the travelling wave regime is complicated and, to date, is
1082 not fully understood. The TWIMS system is, therefore, usually calibrated using ions that have
1083 previously been measured by employing DT-IMS. A typical calibration regime (Knapman et al., 2010)
1084 has been described based on the CCSs of oligo-glycine ions (available at
1085 http://www.indiana.edu/~clemmer/) which are currently accepted to be suitable as they are high
1086 mobility ions in the expected mobility range of small molecules, and have been measured previously
1087 using DT-IMS. Calibration with a static 4 V wave gave more drift time values over a narrower range of
1088 CCSs than a wave ramp, potentially resulting in greater resolving power. Although changes can be
1089 made to the buffer gas used in the measurement, the larger the buffer gas molecules, the larger the
1090 CCS and it was noted that the buffer gas radius used in theoretical calculations must be indicative of
1091 the buffer gas used in the original DT-IMS measurements (typically helium), even if the analysis of
1092 calibrants and analytes is carried out in a different buffer gas.
1093
1094 The experimental resolving power was reported under these conditions for the isomeric amino acids
1095 isoleucine and leucine (131 Da), calculated the CCS at 68.95 Å^2 and 70.51Å^2, respectively from the
1096 measured arrival time distributions (see Figure 34).
1097 .
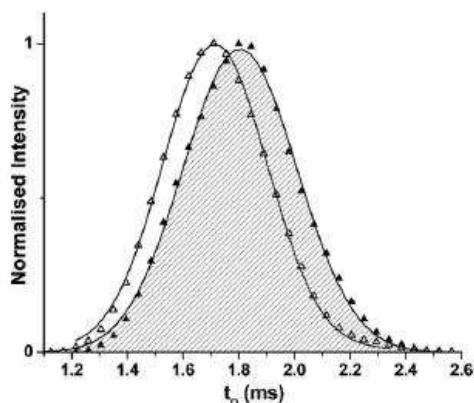
1098
1099 **FIGURE 64.** Overlaid mobility chromatograms of L-Ile (open) and L-Leu (filled) acquired using a static
1100 4 V wave height. The ESI-TWIMS-MS experimental CCS values measured were 68.95 and 70.51Å^2,
1101 and the calculated CCS values were 70.81 and 72.03Å^2, for L-Ile and L-Leu, respectively. Adapted
1102 from Knapman et al., (2010).

1103 To understand the differences between solution state and gas-phase measurements the theoretical
1104 collision cross-sections were calculated as a weighted average over multiple solution-phase rotameric
1105 states from a database of 5000 protein structures and compared to the experimentally measured gas-
1106 phase values (Table 4). Calculated CCS values for hydrophobic amino acids gave the best
1107 agreement with gas-phase TWIMS values, whilst more polar residues are experimentally found to be
1108 much smaller than calculated, mostly likely due to burying of polar and charged termini. The largest
1109 differences also appear to be correlated to the degrees of freedom in the amino acid side-chain.
1110
1111 **TABLE 4.** Comparison of measured and predicted CCS values for seven amino acids, adapted from
1112 Knapman et al., (2010).
1113

Amino acid	Mw (Da)	Rotamers	TWIMS experimental CCS (Å^2)	CCS predicted from solution state (Å^2)	Difference (Å^2)	Notes
Pro	115.12	2	62.43	63.16	0.73	Hydrophobic
Val	117.15	3	64.81	64.82	0.01	Hydrophobic
Leu	131.12	4	70.51	72.03	1.52	Hydrophobic
Ile	131.12	4	68.95	70.81	1.86	Hydrophobic
Asp	133.11	5	62.93	69.81	6.88	Polar

| Gln | 146.15 | 5 | 62.85 | 75.08 | 12.23 | Polar |
| Glu | 147.13 | 7 | 63.35 | 76.69 | 13.34 | Polar |

This demonstrates that IMS-MS can distinguish between subtle changes in shape e.g. differentiating Leu and Ile and also has the potential to reveal structural information about the important interactions present in the gas-phase such as the burial of the polar groups in the examples Gln and Glu.

D. Calculation of collision cross-section (CCS) for small molecules using overtone IMS-MS

Recently, overtone mobility spectrometry (Kurulugama et al., 2009; Valentine et al., 2009), where separation is achieved by applying time-dependent electric fields to sequential segments in a drift-tube thus eliminating ions that are not resonant with the applied field, has been used to demonstrate measurements of ion collision cross-sections:

$$\Omega = \frac{(18\pi)^{1/2}}{16}\frac{ze}{(k_b T)^{1/2}}\left[\frac{1}{m_I}+\frac{1}{m_B}\right]^{1/2}\frac{E[\phi(h-1)+1]}{f(l_t+l_e)}\frac{760}{P}\frac{T}{273.2}\frac{1}{N} \quad (12)$$

where Ω is the collision cross-section, k_b is the Boltzmann constant, z is the ionic charge, e is the charge of an electron, N is the buffer gas density, T is the temperature of the buffer gas, P is the pressure of the buffer gas, E is the electric field, m_I and m_B are the masses of the ion and the buffer gas. The overtone IMS specific parameters include f which is the application frequency, h is the harmonic index, l_t is the ion transmission length and l_e is the ejection length.

Reduced ion mobilities are reported to enable a comparison of DT-IMS-MS and overtone-IMS-MS measurements and are, in general, in good agreement. An especially interesting feature is the potential for overtone-IMS-MS to exclude different ion structures i.e. with different ion mobilities in the IMS stage. Typical IMS and TWIMS approaches are thought to measure an experimental average of all structures sampled within the IMS drift time, whereas overtone-IMS-MS appears to enable selection of particular structures over the IMS drift-time, potentially giving a better understanding of transitions on the IMS measurement timescale, in the order of a few milliseconds. Current measurements are limited for small molecules but development is ongoing.

E. Using theoretical calculations to understand ion mobility data

The assignment of structural information is typically made by comparing theoretical, calculated CCS values with experimentally determined CCS values by using the following procedures:

1. generate list of conformers,
2. minimise structures to lowest energy structures,
3. calculation of theoretical CCS, and
4. comparison of theoretical CCS values with experimentally determined values.

1. Generate list of conformers

Initially the molecule must be transformed from a flat 2D to a representative 3D structure at physiological pH taking into account tautomerism, likely protonation site(s), bond lengths etc. The accessible conformations can be explored for small molecules (Dear et al., 2010; Williams et al., 2009b) using methods including systematic search, molecular dynamics, random search and grid search tools but may be very computationally expensive if the number of rotatable bonds is high, requiring evaluation of thousands of potential structures for relatively simple structures.

2. Minimise structure to lowest energy structures

Molecular dynamics approaches have been applied to small molecules with success and computationally are far less demanding than for large molecules (Baumketner et al., 2006; von Helden et al., 1995; Hoaglund-Hyzer et al., 1999; Jarrold, 2000; Kinnear et al., 2002). Methods have included force-field techniques including MMFF94 forcefield (Dear et al., 2010) and CHARM (Mao et al., 2001) but quantum mechanical methods e.g., density functional theory (DFT) may also be feasible for understanding small molecule structures. Indeed DFT has almost become the 'norm' for

1166 calculating ion structures (Holmes et al., 1985), as it is more accurate than semi-empirical methods .
1167 Recent work (Alex et al., 2009; Wright et al., 2010) has highlighted the potential for DFT to
1168 understand electron density in bond formation/cleavage and the effect of protonation on bond lengths,
1169 which makes DFT a potentially powerful tool in modelling ion structures in IMS-MS. Indeed the
1170 information obtained from DFT calculations may contribute to a better understanding of the ion
1171 structure for both the IMS separation and any tandem MS results.
1172
1173 ### 3. Calculation of theoretical CCS
1174 The main calculation protocols for obtaining theoretical CCS values in IMS include projection
1175 approximation (PA), trajectory method (TJ) and exact hard sphere scattering (EHSS). Whilst there has
1176 been some debate about which type of modelling is most appropriate, it is generally recommended to
1177 use the projection approximation (PA) method for small molecules of 20-100 atoms, for example
1178 using the Sigma software package or MOBCAL software. However, PA typically underestimates
1179 collision cross-sections for polyatomic species, especially for different surfaces including concave
1180 structures, by up to 20% (Shvartsburg and Jarrold, 1996), so is not typically recommended for larger
1181 molecular weight structures.
1182
1183 TJ typically works well for any size system, but calculations are computationally expensive. Exact
1184 Hard Sphere Scattering (EHSS) typically fails with small molecules because the ion-buffer gas
1185 interaction becomes important compared to the geometry of the ion and careful calibration of the
1186 relevant atomic radii is essential (Shvartsburg and Jarrold, 1996). EHSS and TJ appear to provide
1187 better agreement for larger molecular weight ions as the parameterisation of EHSS is based on
1188 fullerenes and other large molecular weight ions.
1189
1190 There have been attempts to improve modelling, for large molecules (Shvartsburg et al., 2007) and
1191 small molecules (Knapman et al., 2010; Siu et al., 2010), by construction of new parameter basis sets
1192 with values for the carbon, oxygen, helium and nitrogen interaction radius calculated from suitable
1193 representative molecules. Further development of modelling and prediction techniques (Fernandez-
1194 Lima et al., 2009) and improvement in parameter basis sets may well provide closer agreement
1195 between calculated and measured CCSs. Recent improvements to a nitrogen based trajectory
1196 method (Campuzano et al. 2011) may help understand data generated in $N_{2(g)}$ (as the less polarizable
1197 $He_{(g)}$ is typically used) and create better calibrations for collision cross sections (especially useful in
1198 TWIMS where $N_{2(g)}$ is the typical drift gas). The set of collision cross sections for pharmaceutically
1199 relevant 'small molecule' compounds appears self consistent (R^2 = 0.9949) and covers a useful range
1200 of 124.5 to 254.3 $Å^2$ for nitrogen gas and a range of 63.0 to 178.8 $Å^2$ for helium gas.
1201
1202 ### 4. Comparison of calculated CCS values with experimentally determined values
1203 Typically validation is best achieved using known standards within experimental sets, either for
1204 relative ranking of results or to increase confidence in measurements. Structure co-ordination sets are
1205 widely available for some species e.g. at the RCSB Protein Data Bank and have been data based by
1206 Clemmer (available at
1207 http://www.indiana.edu/%7eclemmer/Research/cross%20section%20database/Proteins/protein_cs.ht
1208 m). However, it should be noted that the co-ordination structures from different sources may not agree
1209 as NMR structures are often subject to solvent effects, x-ray structures subject to crystal lattice effects
1210 and measurements by ion mobility may be subject to gas-phase neutral contamination, ionisation and
1211 solvent effects. Some publications describe the calculation of theoretical collision-cross sections using
1212 datasets obtained from NMR and x-ray files (e.g. PDB files) as input without subsequent energy
1213 minimisation in the gas-phase which could result in erroneous estimates of CCS and further
1214 assignment; in such a case a better understanding via structure/energy minimisation may be
1215 important.

1216 # VI. PREDICTION OF ION MOBILITY CONSTANTS
1217 Whilst many approaches to IMS explicitly use or attempt to derive information on the 3D structure of
1218 the ion another approach is to use molecular descriptors to adequately describe an ion and predict
1219 the reduced mobility without any requirement to carry out computationally expensive geometry
1220 optimisation. A quantitative structure property relationship (QSPR) methodology using five
1221 descriptors for a training set of 70 organic compounds and excluding three outliers gave a multi-linear
1222 regression (MLR) of R^2 = 0.98 and s = 0.047; the test set of seven compounds gave s = 0.047
1223 (Wessel and Jurs, 1994). Later, using six molecular descriptors on a training set of 135 compounds
1224 and testing the model with 18 compounds gave an RMS error of 0.038 (Wessel et al., 1996). A more

1225 diverse set of 182 compounds and modification of two of the descriptors correlated with an R^2 =0.80
1226 (Agbonkonkon et al., 2004). A subset of 159 of that data set was used to develop linear and non-
1227 linear models using MLR and progression pursuit regression to achieve R^2 values of 0.908 and 0.938
1228 and s = 0.066 and 0.055, respectively (Liu et al., 2007a). The recent formulation of a linear equation
1229 for ion mobility in a series of polar aliphatic organic compounds resulted in ion mobility predictions that
1230 were typically >99% accurate (Hariharan et al., 2010).
1231
1232 These molecular descriptor approaches are now widely used in predicting peptide IMS-MS drift times
1233 (Wang et al., 2010) to improve confidence in peptide identification. The same approach to prediction
1234 of 'small molecule' IMS-MS drift times could well help refine models of drift time prediction and better
1235 understand important interactions affecting drift time and thus gas-phase structures, however this is
1236 currently not well understood.

VII. FUTURE DEVELOPMENTS

1237
1238 The adoption of IMS-MS both for small molecule as well as large molecule applications is likely to
1239 continue strongly, assisted by rapid developments in IMS design that marries the two stages of IMS
1240 and MS and mitigates the challenges of ion efficiency and resolution that has hindered their
1241 combination.
1242
1243 The resistive glass-IMS design recently invented to replace the traditional stacked-ring ion guides
1244 enables easier construction (Kwasnik and Fernández, 2010) and designs include a segmented rf
1245 quadrupole in the vacuum interface that improve sensitivity by over 2 order of magnitude (Kaplan et
1246 al., 2010). The inverse ion mobility spectrometry technique that applies an inverted pulse to the
1247 shutter grid appears to increase resolution by 30-60% presumably by creating a gap in the charge
1248 cloud and thus reducing space-charging effects (Tabrizchi and Jazan, 2010).
1249
1250 A further hyphenation of a photoelectron spectrometer to a IMS-TOFMS shows promise as a
1251 complementary method to obtain further information on the structures of gas-phase ions by obtaining
1252 photoelectron spectra at three different detachment laser wavelengths (Vonderach et al., 2011), and
1253 also hints at the possibilities for further information-rich data to be acquired and combined with IMS-
1254 MS by further hypenation.
1255
1256 The adoption of IMS in hyphenated IMS-MS systems is continuing with important developments, for
1257 example, Agilent previously announced collaborations with Owlstone Nanotechnologies for an IMS-
1258 MS system and Bruker have investigated new modes of IMS (Baykut et al., 2009). There have been
1259 long-term research investments demonstrated in the launch of the second generation Waters Synapt
1260 G2 IMS-MS with improved resolution and ion transmission and with the AB Sciex SelexION
1261 technology that is available for the AB Sciex Triple Quad 5500 and QTRAP 5500 Systems including
1262 selection of gas-phase dopants which can improve IMS separation and rapid 25 ms cycle time per
1263 MRM which matches cycle times with multi-component analysis and UHPLC time scales.
1264

VIII. CONCLUSIONS

1265
1266 Whilst IMS is a ubiquitous technique in airports as well as military and forensic applications, it is still
1267 the case that using IMS-MS for measuring structural information and for separations in 'small
1268 molecule' applications there are subtle differences that can significantly affect the mobility and there is
1269 much more to be understood about how to measure the structures of gas-phase ions reliably, the
1270 nature of the fundamental intra-molecular interactions that define the structures and what the effect of
1271 ion-neutral interactions are on ion mobility.
1272
1273 Many chemical classes have been investigated using IMS and IMS-MS and some of the main
1274 publications are listed in Table 5 to direct the reader to more detail on those classes.

1275 *TABLE 5.* Applications of IMS-MS and IMS to 'small molecule' classes.

1276

Class	Year
Hydrocarbons (Creaser et al., 2004)	1973
Halogenated benzenes and nitro benzenes (o-, m-substituted) (Karpas et al., 1988)	1973
Dihalogenated benzenes (o-, m-substituted) (Karpas et al., 1988)	1974

Benzoic and isophthalic and phthalic acids (Karpas et al., 1988)	1975
Some sec-butylcholorodiphenyl oxides (Karpas et al., 1988)	1976
o- and p- substituted chlorodiphenyl oxides (Karpas et al., 1988)	1976
Ethyl butyl esters of maleic and fumaric (Karpas et al., 1988)	1982
Succinic acids (Karpas et al., 1988)	1982
Isomeric ketones 2-octanone vs. 4,4-dimethyl-3-hexanone (Karpas et al., 1988)	1986
Isomeric alcohols 1-octanol vs. 2-octanol (Karpas et al., 1988)	1986
Substituted electrophilic olefins, keto enol isomers, 2 keto and 2 enol (Karpas et al., 1988)	1988
Amides and amines (Karpas et al., 1988) (Karpas et al., 1994)	1989 & 1994
Anilines (Karpas et al., 1990b)	1990
Simple monocyclic and dicyclic compounds (Karpas et al., 1990a)	1990
Aminoazoles (Karpas and Tironi, 1991)	1991
Ketones (Karpas, 1991)	1991
Aminoalcohols (Karpas, 1992)	1991
Benzodiazepines, amphetamines and opiates (Karpas et al., 1988)	2001 & 2002
Amino acids (Asbury & Hill, 2000b)	2001
Amphetamines (Matz and Hill, 2002)	2002

1277
1278   Standardized calibration and measurement methods (Fernández-Maestre et al., 2010b), easily
1279   implemented and accurate predictive models and interpretation of results are still being developed but
1280   show great promise. The interchange between academia, vendors and industry is ensuring more
1281   options are available to potential users of IMS-MS. A range of current commercial manufacturers and
1282   IMS-MS types are listed in Table 6 for reference.

1283   **TABLE 6.** Commercially available IMS systems, or accessories able to interface to MS systems.

IMS-MS manufacturer	Type
Excellims IMS-MS	DT-IMS
Tofwerk IMS-MS	DT-IMS
Waters Synapt IMS-MS	TWIMS
Thermo FAIMS cylindrical electrode	FAIMS
Owlstone Nanotech	FAIMS
AB Sciex SelexION parallel plate	DMS
Sionex microDMx	DMS

1284
1285   Over the last decade there have been many novel applications and developments in IMS-MS
1286   involving new methods to generate ions, accumulate and focus ions, select ions preferentially,
1287   measure and process the multiplexed information and they have been used to solve problems ranging
1288   from hydration/desolvation in 'small' organic molecules to understanding the fundamental interactions
1289   in the building blocks of life, amino acids. IMS-MS is a novel method that can separate ions and use
1290   information on their mobility to assign structure on an unparalleled rapid timeframe and at high levels
1291   of sensitivity. In combination with a range of analytical equipment including ionisation sources,
1292   separation devices, solution chemistry and gas-phase chemistry; the use of IMS-MS offers a versatile
1293   and powerful approach to unique insights into complex mixtures and hitherto ambiguous structures.
1294
1295
1296   **REFERENCES**
1297
1298   Agbonkonkon N, Tolley HD, Asplund MC, Lee ED, Lee ML. 2004. Prediction of gas-phase reduced
1299   ion mobility constants (K0). Anal Chem 76:5223-5229.
1300   Aksenov AA, Kapron JT. 2010. Behaviour of tetraalkylammonium ions in high-field asymmetric
1301   waveform ion mobility spectrometry. Rapid Commun Mass Spectrom 24:1392-1396.
1302   Albritton DL, Miller TM, Martin DW, McDaniel EW. 1968. Mobilities of mass-identified H_3^+ and H^+ ions
1303   in hydrogen. Phys Rev 171:94.
1304   Alex A, Harvey S, Parsons T, Pullen FS, Wright P, Riley, JA. (2009). Can density functional theory
1305   (DFT) be used as an aid to a deeper understanding of tandem mass spectrometric
1306   fragmentation pathways?. Rapid Commun Mass Spectrom, 23: 2619–2627

Allen FH, Harris SE, Taylor R. 1996. Comparison of conformer distributions in the crystalline state with conformational energies calculated by *ab initio* techniques. J Comput-Aid Mol Des 10:247-254.

Alonso R, Rodríguez-Estévez V, Domínguez-Vidal A, Ayora-Cañada MJ, Arce L, Valcárcel M. 2008. Ion mobility spectrometry of volatile compounds from iberian pig fat for fast feeding regime authentication. Talanta 76:591-596.

Project Summary. . Recovery.gov. http://www.recovery.gov/Transparency/RecipientReportedData/pages/RecipientProjectSummary508.aspx?AwardIDSUR=93260&qtr=2010Q3.

Arthur KE, Wolff J. Carrier DJ. 2004. Analysis of betamethasone, dexamethasone and related compounds by liquid chromatography/electrospray mass spectrometry. Rapid Commun Mass Spectrom 18: 678-684

Asbury GR, Hill HH. 2000a. Evaluation of ultrahigh resolution ion mobility spectrometry as an analytical separation device in chromatographic terms. J. Micro Sep 12:172-178.

Asbury GR, Hill HH. 2000b. Separation of amino acids by ion mobility spectrometry. J Chromatog A 902:433-437.

Asbury GR, Hill HH. 2000c. Using Different Drift Gases To Change Separation Factors (α) in Ion Mobility Spectrometry. Anal. Chem.72: 580-584

Aston FW. 1919. A positive ray spectrograph. Philos. Mag., 38: 707-715.

Baim MA, Hill HH. 1982. Tunable selective detection for capillary gas chromatography by ion mobility monitoring. Anal Chem 54:38-43.

Baker ES, Bushnell JE, Wecksler SR, Lim MD, Manard MJ, Dupuis NF, Ford PC, Bowers MT. 2005. Probing shapes of bichromophoric metal−organic complexes using ion mobility mass spectrometry. J Am Chem Soc 127:18222-18228.

Barnes WS, Martin DW, McDaniel EW. 1961. Mass spectrographic identification of the ion observed in hydrogen mobility experiments. Phys. Rev Lett 6:110.

Bastug T, Kuyucak S. 2003. Role of the dielectric constants of membrane proteins and channel water in ion permeation. Biophys J 84:2871-2882.

Baumketner A, Bernstein SL, Wyttenbach T, Lazo ND, Teplow DB, Bowers MT, Shea J-E. 2006. Structure of the 21-30 fragment of amyloid β-protein. Protein Sci 15:1239-1247.

Baykut G, von Halem O, Raether O. 2009. Applying a Dynamic Method to the Measurement of Ion Mobility. J Am Soc Mass Spectrom, 20: 2070-2081

Beegle LW, Kanik I, Matz L, Hill HH. 2001. Electrospray ionization high-resolution ion mobility spectrometry for the detection of organic compounds, 1. amino acids. Anal Chem 73:3028-3034.

Belov ME, Clowers BH, Prior DC, Danielson III WF, Liyu AV, Petritis BO, Smith RD. 2008. Dynamically multiplexed ion mobility time-of-flight mass spectrometry. Anal Chem 80:5873-5883.

Bluhm BK, Gillig KJ, Russell DH. 2000. Development of a fourier-transform ion cyclotron resonance mass spectrometer-ion mobility spectrometer. Rev Sci Instrum 71:4078.

Bohrer BC, Merenbloom SI, Koeniger SL, Hilderbrand AE, Clemmer DE. 2008. Biomolecule analysis by ion mobility spectrometry. Ann Rev Anal Chem 1:293-327.

Budimir N, Weston DJ, Creaser CS. 2007. Analysis of pharmaceutical formulations using atmospheric pressure ion mobility spectrometry combined with liquid chromatography and nano-electrospray ionisation. Analyst 132:34.

Buryakov IA, Krylov EV, Nazarov EG, Rasulev UK. 1993. A new method of separation of multi-atomic ions by mobility at atmospheric pressure using a high-frequency amplitude-asymmetric strong electric field. Int J Mass Spectrom. 128:143-148

Canterbury JD, Yi X, Hoopmann MR, MacCoss MJ. 2008. Assessing the dynamic range and peak capacity of nanoflow lc−faims−ms on an ion trap mass spectrometer for proteomics. Anal Chem 80:6888-6897.

Campuzano I, Bush MF, Robinson CV, Beaumont C, Richardson K, Kim H, Kim HI. 2012. Structural Characterization of Drug-like Compounds by Ion Mobility Mass Spectrometry: Comparison of Theoretical and Experimentally Derived Nitrogen Collision Cross Sections. Anal Chem 84 (2):1026–1033.

Champarnaud E, Laures AM-F, Borman PJ, Chatfield MJ, Kapron JT, Harrison M, Wolff J-C. 2009. Trace level impurity method development with high-field asymmetric waveform ion mobility spectrometry: systematic study of factors affecting the performance. Rapid Commun Mass Spectrom 23:181-193.

1366 Clemmer DE. 1997. Injected-ion mobility analysis of biomolecules.
1367   http://www.indiana.edu/~clemmer/Publications/pub%20042.pdf.
1368 Clowers BH, Ibrahim YM, Prior DC, Danielson WF, Belov ME, Smith RD. 2008. Enhanced ion
1369   utilization efficiency using an electrodynamic ion funnel trap as an injection mechanism for ion
1370   mobility spectrometry. Anal. Chem 80:612-623.
1371 Clowers BH, Hill HH. 2006. Influence of cation adduction on the separation characteristics of flavonoid
1372   diglycoside isomers using dual gate-ion mobility-quadrupole ion trap mass spectrometry. J
1373   Mass Spectrom 41:339-351.
1374 Clowers BH, Siems WF, Hill HH, Massick SM. 2006. Hadamard transform ion mobility spectrometry.
1375   Anal Chem 78:44-51.
1376 Collins DC, Lee ML. 2001. Electrospray ionization gas-phase electrophoresis under ambient
1377   conditions and it's potential or high-speed separations. Fresenius' J Anal Chem 369:225-233.
1378 Covey T, Douglas DJ. 1993. Collision cross sections for protein ions. J. Am. Soc. Mass Spectrom.4:
1379   616-623

1381 Coy SL, Krylov EV, Schneider BB, Covey TR, Brenner DJ, Tyburski JB, Patterson AD, Krausz KW,
1382   Fornace AJ, Nazarov EG.2010.Detection of Radiation-Exposure Biomarkers by Differential
1383   Mobility Prefiltered Mass Spectrometry (DMS-MS). Int. J. Mass Spectrom.. 291: 108-117
1384 Creaser CS, Benyezzar M, Griffiths JR, Stygall JW. 2000. A tandem ion trap/ion mobility spectrometer.
1385   Anal Chem 72:2724-2729.
1386 Creaser CS, Griffiths JR, Bramwell CJ, Noreen S, Hill CA, Thomas CLP. 2004. Ion mobility
1387   spectrometry: a review. part 1. structural analysis by mobility measurement. Analyst 129:984.
1388 Cui M, Ding L, Mester Z. 2003. Separation of cisplatin and its hydrolysis products using electrospray
1389   ionization high-field asymmetric waveform ion mobility spectrometry coupled with ion trap
1390   mass spectrometry. Anal Chem 75:5847-5853.
1391 Cuyckens F, Wassvik C, Mortishire‑Smith RJ, Tresadern G, Campuzano I, Claereboudt J. 2011.
1392   Product ion mobility as a promising tool for assignment of positional isomers of drug
1393   metabolites. Rapid Commun Mass Spectrom. 25:3497-3503
1394 D'Agostino PA, Chenier CL. 2010. Desorption electrospray ionization mass spectrometric analysis of
1395   organophosphorus chemical warfare agents using ion mobility and tandem mass
1396   spectrometry. Rapid Commun Mass Spectrom 24:1617-1624.
1397 Dear GJ, Munoz-Muriedas J, Beaumont C, Roberts A, Kirk J, Williams JP, Campuzano I. 2010. Sites
1398   of metabolic substitution: investigating metabolite structures utilising ion mobility and
1399   molecular modelling. Rapid Commun Mass Spectrom 24:3157-3162.
1400 de la Mora JF, Ude S, Thomson BA. 2006. The potential of differential mobility analysis coupled to
1401   MS for the study of very large singly and multiply charged proteins and protein complexes in
1402   the gas phase. Biotechnol. J. 1: 988-997
1403 Douglas DH. 1998. Applications of Collision Dynamics in Quadrupole Mass Spectrometry. J Am Soc
1404   Mass Spectrom. 9: 101-113
1405 Dussy FE, Berchtold C, Briellmann TA, Lang C, Steiger R, Bovens M. 2008. Validation of an ion
1406   mobility spectrometry (ims) method for the detection of heroin and cocaine on incriminated
1407   material. Forensic Sci Int 177:105-111.
1408 Dwivedi P, Bendiak B, Clowers BH, Hill HH. 2007. Rapid resolution of carbohydrate isomers by
1409   electrospray ionization ambient pressure ion mobility spectrometry-time-of-flight mass
1410   spectrometry (esi-apims-tofms). J Am Soc Mass Spectrom 18:1163-1175.
1411 Dwivedi P, Schultz AJ, Jr HHH. 2010. Metabolic profiling of human blood by high-resolution ion
1412   mobility mass spectrometry (im-ms). Int J Mass Spectrom 298:78-90.
1413 Dwivedi P, Wu C, Matz LM, Clowers BH, Siems WF, Hill HH. 2006. Gas-phase chiral separations by
1414   ion mobility spectrometry. Anal Chem 78:8200-8206.
1415 Eatherton RL, Morrissey MA, Siems WF, Hill HH. 1986. Ion mobility detection after supercritical fluid
1416   chromatography. J High Res Chromatogr 9:154-160.
1417 Eiceman GA, Karpas Z. 2004. Ion mobility spectrometry. 2nd edition. Boca Raton, FL, USA: CRC
1418 Press
1419 Eiceman GA, Yuan-Feng W, Garcia-Gonzalez L, Harden CS, Shoff DB. 1995. Enhanced selectivity in
1420   ion mobility spectrometry analysis of complex mixtures by alternate reagent gas chemistry.
1421   Anal Chim Acta 306:21-33.
1422 Eiceman GA, Krylov EV, Krylova NS, Nazarov EG, Miller RA. 2004. Separation of Ions from
1423   Explosives in Differential Mobility Spectrometry by Vapor-Modified Drift Gas. Anal. Chem. 76:
1424   4937-4944

1425 Enders JR, Mclean JA. 2009. Chiral and structural analysis of biomolecules using mass spectrometry
1426   and ion mobility - mass spectrometry. Chirality 21:E253-E264.
1427 Fenn LS, McLean JA. 2008. Enhanced carbohydrate structural selectivity in ion mobility-mass
1428   spectrometry analyses by boronic acid derivatization. Chem. Comm. 13:5505-5507
1429 Fernandez-Lima FA, Wei H, Gao YQ, Russell DH. 2009. On the structure elucidation using ion
1430   mobility spectrometry and molecular dynamics. J Phys Chem A 113:8221-8234.
1431 Fernández-Maestre R, Wu C, Hill Jr. HH. 2010. Using a buffer gas modifier to change separation
1432   selectivity in ion mobility spectrometry Int J Mass Spectrom 298:2-9.
1433 Fernandez-Maestre R, Harden CS, Ewing RG, Crawford CL, Hill Jr. HH. 2010. Chemical standards in
1434   ion mobility spectrometry. The Analyst.135:1433-1442
1435 Foloppe N, Chen I-J. 2009. Conformational sampling and energetics of drug-like molecules. Curr.
1436   Med Chem 16:3381-3413.
1437 Gehrke CW. 2001. Chromatography: a century of discovery 1900-2000: the bridge to the
1438   sciences/technology. Boca Raton, FL, USA: Elsevier.
1439 Gerlich D. 1992 In: State-Selected and State-to-State Ion-Molecule Reaction Dynamics. Part 1. Ng
1440   CY, Baer M, editors. LXXXII. John Wiley; New York: pp. 1–176
1441 Giles K, Wildgoose JL, Langridge DJ, Campuzano I. 2010. A method for direct measurement of ion
1442   mobilities using a travelling wave ion guide. Int J Mass Spectrom 298:10-16
1443 Giles K, Williams JP, Campuzano I. 2011. Enhancements in travelling wave ion mobility resolution.
1444   Rapid Comm Mass Spectrom 25:1559-1566.
1445 Gorshkov MP. 1982. Inventor's certificate USSR no. 966583 Byull Izobret 38.
1446 Griffin GW, Dzidic I, Carroll DI, Stillwell RN, Horning EC. 1973. Ion mass assignments based on
1447   mobility measuremets. validity of plasma chromatographic mass mobility correlations. Anal
1448   Chem 45:1204-1209.
1449 Guevremont R, Purves RW. 1999. Atmospheric pressure ion focusing in a high-field asymmetric
1450   waveform ion mobility spectrometer. Rev. Sci. Instrum. 70: 1370-1384
1451 Guo Y, Wang J, Javahery G, Thomson BA, Siu KWM. 2004. Ion Mobility Spectrometer with Radial
1452   Collisional Focusing. Anal. Chem. 77:266-275
1453 Guo Y, Srinivasan S, Gaiki S. 2009. Evaluation of the peak capacity of various rp-columns for small
1454   molecule compounds in gradient elution. Chromatographia 70:1045-1054.
1455 Hariharan CB, Baumbach JI, Vautz W. 2010. Linearized equations for the reduced ion mobilities of
1456   polar aliphatic organic compounds. Anal Chem 82:427-431.
1457 Harry EL, Reynolds JC, Bristow AWT, Wilson ID, Creaser CS. 2009. Direct analysis of pharmaceutical
1458   formulations from non-bonded reversed-phase thin-layer chromatography plates by
1459   desorption electrospray ionisation ion mobility mass spectrometry. Rapid Commun Mass
1460   Spectrom 23:2597-2604.
1461 Harry EL, Bristow AWT, Wilson ID, Creaser CS. 2011. Real-time reaction monitoring using ion
1462   mobility-mass spectrometry. Analyst 136:1728.
1463 Harvey SR, MacPhee CE, Barran PE, 2011. Ion mobility mass spectrometry for peptide analysis,
1464 Methods, 54, 4: 454-461
1465 Hatsis P, Brockman AH, Wu J-T. 2007. Evaluation of high-field asymmetric waveform ion mobility
1466   spectrometry coupled to nanoelectrospray ionization for bioanalysis in drug discovery. Rapid
1467   Commun Mass Spectrom 21:2295-2300.
1468 Heck AJR, van den Heuvel RHH. 2004. Investigation of intact protein complexes by mass
1469   spectrometry. Mass Spectrom Rev 23:368-389.
1470 von Helden G, Wyttenbach T, Bowers MT. 1995. Conformation of macromolecules in the gas phase:
1471   use of matrix-assisted laser desorption methods in ion chromatography. Science 267:1483-
1472   1485.
1473 Henderson SC, Valentine SJ, Counterman AE, Clemmer DE. 1999. Esi/ion trap/ion mobility/time-of-
1474   flight mass spectrometry for rapid and sensitive analysis of biomolecular mixtures. Anal Chem
1475   71:291-301.
1476 Hill CA, Thomas CLP. 2003. A pulsed corona discharge switchable high resolution ion mobility
1477   spectrometer-mass spectrometer. Analyst 128:55-60.
1478 Hoaglund-Hyzer CS, Counterman AE, Clemmer DE. 1999. Anhydrous protein ions. Chem Rev
1479   99:3037-3080.
1480 Hogan CJ, Ruotolo BT, Robinson CV, Fernandez de la Mora J. 2011. Tandem Differential Mobility
1481   Analysis-Mass Spectrometry Reveals Partial Gas-Phase Collapse of the GroEL ComplexJ.
1482   Phys. Chem. B.115:3614-3621

1483   Hogg AM, Kebarle P. 1965 Mass-Spectrometric Study of Ions at Near-Atmospheric Pressure. II.
1484   Ammonium Ions Produced by the Alpha Radiolysis of Ammonia and Their Solvation in the
1485   Gas Phase by Ammonia and Water Molecules. J. Chem. Phy. 43:449-457
1486   Holmes JL. 2006. Assigning structures to ions in the gas phase. New York: CRC Press.
1487   Homans SW. 2007. Water, water everywhere--except where it matters? Drug Discov Today 12:534-
1488   539.
1489   Howdle MD, Eckers C, Laures AM-F, Creaser CS. 2009. The use of shift reagents in ion mobility-
1490   mass spectrometry: studies on the complexation of an active pharmaceutical ingredient with
1491   polyethylene glycol excipients. J Am Soc Mass Spectrom 20:1-9.
1492   Howdle MD, Eckers C, Laures AM-F, Creaser CS. 2010. The effect of drift gas on the separation of
1493   active pharmaceutical ingredients and impurities by ion mobility-mass spectrometry. Int J
1494   Mass Spectrom 298:72-77.
1495   Huang MX, Markides KE, Lee ML. 1991. Evaluation of an ion mobility detector for supercritical fluid
1496   chromatography with solvent-modified carbon dioxide mobile phases. Chromatographia
1497   31:163-167.
1498   Ibrahim YM, Meot-Ner M, Alshraeh EH, El-Shall MS, Scheiner S. 2005. Stepwise hydration of ionized
1499   aromatics. energies, structures of the hydrated benzene cation, and the mechanism of
1500   deprotonation reactions. J Am Chem Soc 127:7053-7064.
1501   Jackson SN, Ugarov M, Egan T, Post JD, Langlais D, Schultz JA, Woods AS. 2007. Maldi-ion
1502   mobility-tofms imaging of lipids in rat brain tissue. J Mass Spectrom 42:1093-1098.
1503   Jafari MT, Khayamian T, Shaer V, Zarei N. 2007. Determination of veterinary drug residues in chicken
1504   meat using corona discharge ion mobility spectrometry. Anal Chim Acta 581:147-153.
1505   Jafari MT. 2006. Determination and identification of malathion, ethion and dichlorovos using ion
1506   mobility spectrometry. Talanta 69:1054-1058.
1507   Javahery G, Thomson B. 1997. A segmented radiofrequency-only quadrupole collision cell for
1508   measurements of ion collision cross section on a triple quadrupole mass spectrometer. J. Am.
1509   Soc. Mass Spectrom. 8:697-702
1510   Jarrold MF. 2000. Peptides and proteins in the vapor phase. Annu Rev Phys Chem 51:179-207.
1511   Jurneczko E, Barran PE. 2011. How useful is ion mobility mass spectrometry for structural biology?
1512   the relationship between protein crystal structures and their collision cross sections in the gas
1513   phase. Analyst 136:20.
1514   Kanu AB, Dwivedi P, Tam M, Matz L, Hill HH. 2008. Ion mobility-mass spectrometry. J. Mass
1515   Spectrom 43:1-22.
1516   Kaplan K, Graf S, Tanner C, Gonin M, Fuhrer K, Knochenmuss R, Dwivedi P, Hill HH. 2010. Resistive
1517   glass im-tofms. Anal Chem 82:9336-9343.
1518   Karasek FW, Hill HH, Kim SH. 1976. Plasma chromatography of heroin and cocaine with mass-
1519   identified mobility spectra. J Chromatogr 117:327-336.
1520   Karimi A, Alizadeh N. 2009. Rapid analysis of captopril in human plasma and pharmaceutical
1521   preparations by headspace solid phase microextraction based on polypyrrole film coupled to
1522   ion mobility spectrometry. Talanta 79:479-485.
1523   Karpas Z, Bell SE, Wang Y-F, Walsh M, Eiceman GA. 1994. The structure of protonated diamines
1524   and polyamines. Struct Chem 5:135-140.
1525   Karpas Z. 1991. The structure and mobility in air of protonated ketones. Int J Mass Spectrom
1526   107:435-440.
1527   Karpas Z. 1992. The mobility of protonated aminoalcohols: evidence for proton-induced cyclization.
1528   Struct Chem 3:139-141.
1529   Karpas Z, Berant Z, Shahal O. 1990. The effects of saturation and substitution on the mobility of
1530   protonated cyclic compounds. Int J Mass Spectrom Ion Proc 96:291-297.
1531   Karpas Z, Berant Z, Stimac RM. 1990. An ion mobility spectrometry/mass spectrometry (ims/ms)
1532   study of the site of protonation in anilines. Struct Chem 1:201-204.
1533   Karpas Z, Stimac RM, Rappoport Z. 1988. Differentiating between large isomers and derivation of
1534   structural information by ion mobility spectrometry / mass spectrometry techniques. Int J Mass
1535   Spectrom Ion Proc 83:163-175.
1536   Karpas Z, Tironi C. 1991. The mobility and ion structure of protonated aminoazoles. Struct Chem
1537   2:655-659.
1538   Kebarle P, Hogg AM. 1965. Mass-Spectrometric Study of Ions at Near Atmospheric Pressures. I. The
1539   Ionic Polymerization of Ethylene. The Journal of Chemical Physics. 42: 668-675
1540   Keller T, Keller A, Tutsch-Bauer E, Monticelli F. 2006. Application of ion mobility spectrometry in
1541   cases of forensic interest. Forensic Sci Int 161:130-140.

1542 Kemper PR, Dupuis NF, Bowers MT. 2009. A new, higher resolution, ion mobility mass spectrometer.
1543   Int J Mass Spectrom 287:46-57.
1544 Kinnear BS, Hartings MR, Jarrold MF. 2002. The energy landscape of unsolvated peptides: helix
1545   formation and cold denaturation in ac-a4g7a4 + h+. J Am Chem Soc 124:4422-4431.
1546 Knapman TW, Berryman JT, Campuzano I, Harris SA, Ashcroft AE. 2010. Considerations in
1547   experimental and theoretical collision cross-section measurements of small molecules using
1548   travelling wave ion mobility spectrometry-mass spectrometry. Int J Mass Spectrom 298: 17-23.
1549 Knutson E, Whitby K. 1975. Aerosol classification by electric mobility: Apparatus, theory, and
1550   applications. J. Aerosol Sci. 6 (6): 443–451Koeniger SL, Merenbloom SI, Clemmer DE. 2006.
1551   Evidence for many resolvable structures within conformation types of electrosprayed ubiquitin
1552   ions. J Phys Chem B 110:7017-7021.
1553 Kolakowski BM, Mester Z. 2007. Review of applications of high-field asymmetric waveform ion
1554   mobility spectrometry (faims) and differential mobility spectrometry (dms). Analyst 132:842-
1555   864.
1556 Krylov EV. 1999. A method of reducing diffusion losses in a drift spectrometer. Tech Phys+. 44:113-
1557   116
1558 Krylov E, Nazarov EG, Miller RA, Tadjikov B, Eiceman GA. 2002. Field Dependence of Mobilities for
1559   Gas-Phase-Protonated Monomers and Proton-Bound Dimers of Ketones by Planar Field
1560   Asymmetric Waveform Ion Mobility Spectrometer (PFAIMS). J. Phys. Chem. A. 106:5437-
1561   5444
1562 Krylov EV. 2003. Comparison of the planar and coaxial field asymmetrical waveform ion mobility
1563   spectrometer (FAIMS). Int. J. Mass Spectrom. 225:39-51
1564 Krylov EV, Nazarov EG. 2009. Electric field dependence of the ion mobility. Int. J. Mass Spectrom.
1565   285:149-156
1566 Kurulugama RT, Nachtigall FM, Lee S, Valentine SJ, Clemmer DE. 2009. Overtone mobility
1567   spectrometry: part 1. experimental observations. J Am Soc Mass Spectrom 20:729-737.
1568 Kwasnik M, Fernández FM. 2010. Theoretical and experimental study of the achievable separation
1569   power in resistive-glass atmospheric pressure ion mobility spectrometry. Rapid Commun Mas
1570   Spectrom 24:1911-1918.
1571 Langevin P. 1905. Une formule fondamentale de théorie cinétique. Ann Chim Phys 5:245.
1572 Lawrence AH. 1986. Ion mobility spectrometry/mass spectrometry of some prescription and illicit
1573   drugs. Anal Chem 58:1269-1272.
1574 Levin DS, Vouros P, Miller RA, Nazarov EG, Morris JC. 2004. Characterization of Gas-Phase
1575   Molecular Interactions on Differential Mobility Ion Behavior Utilizing an Electrospray
1576   Ionization-Differential Mobility-Mass Spectrometer System. Anal. Chem.78: 96-106
1577 Levin DS, Vouros P, Miller RA, Nazarov EG. 2007. Using a nanoelectrospray-differential mobility
1578   spectrometer-mass spectrometer system for the analysis of oligosaccharides with solvent
1579   selected control over esi aggregate ion formation. J Am Soc Mass Spectrom 18:502-511
1580 Li X, Stoll DR, Carr PW. 2009. Equation for peak capacity estimation in two-dimensional liquid
1581   chromatography. Anal Chem 81:845-850.
1582 Likar MD, Cheng G, Mahajan N, Zhang Z. 2011. Rapid identification and absence of drug tests for ag-
1583   013736 in 1 mg axitinib tablets by ion mobility spectrometry and dart(tm) mass spectrometry.
1584   J Pharm Biomed Anal 55:569-573.
1585 Lipinski CA, Lombardo F, Dominy BW, Feeney PJ. 1997. Experimental and computational
1586   approaches to estimate solubility and permeability in drug discovery and development
1587   settings. Adv Drug Del Rev 23:3-25.
1588 Liu H, Yao X, Liu M, Hu Z, Fan B. 2007a. Prediction of gas-phase reduced ion mobility constants (k(0))
1589   based on the multiple linear regression and projection pursuit regression. Talanta 71:258-263.
1590 Liu X, Valentine SJ, Plasencia MD, Trimpin S, Naylor S, Clemmer DE. 2007b. Mapping the human
1591   plasma proteome by scx-lc-ims-ms. J Am Soc Mass Spectrom 18:1249-1264.
1592 Maitra U, Bag BG, Rao P, Powell D. 1995. Asymmetric synthesis of steroidal Troger's base analogues.
1593   X-ray molecular structure of methyl 3α,12α-{6H,12H-5,11-methanodibenzo[b,f][1,5]diazocine-
1594   2,8-bisacetoxy}-5β-cholan-24-oate. J. Chem. Soc. Perkin Trans. 1:2049
1595 Manard MJ, Trainham R, Weeks S, Coy SL, Crylov EV, Nazarov EG. 2010. Differential mobility
1596   spectrometry/mass spectrometry: The design of a new mass spectrometer for real-time
1597   chemical analysis in the field. Int J Mass Spectrom 295: 138-144
1598 Mao Y, Ratner MA, Jarrold MF. 2001. Molecular dynamics simulations of the rehydration of folded
1599   and unfolded cytochrome c ions in the vapor phase. J Am Chem Soc 123:6503-6507.

Martínez-Lozano P, Rus J. 2010. Separation of Isomers L-Alanine and Sarcosine in Urine by Electrospray Ionization and Tandem Differential Mobility Analysis-Mass Spectrometry. J Am Soc Mass Spectrom. 21(7): 1129-1132

Martínez-Lozano P, Criado E, Vidal G, Cristoni S, Franzoso F, Piatti M, Brambilla P. 2011. Differential mobility analysis-mass spectrometry coupled to XCMS algorithm as a novel analytical platform for metabolic profiling. Metabolomics. 1-14

Mason EA, McDaniel EW, 1988. Transport Properties of Ions in Gases, New York: John Wiley & Sons, 560p

Matz LM, Hill HH. 2002a. Evaluating the separation of amphetamines by electrospray ionization ion mobility spectrometry/ms and charge competition within the ESI process. Anal Chem 74:420-427.

Matz LM, Hill HH, Beegle LW, Kanik I. 2002b. Investigation of drift gas selectivity in high resolution ion mobility spectrometry with mass spectrometry detection. J Am Soc Mass Spectrom 13:300-307.

McAfee KB, Edelson D. 1963. Identification and mobility of ions in a Townsend discharge by time-resolved mass spectrometry. Proc Phys Soc 81:382-384.

McDaniel EW, Martin DW. 1960. Drift tube-mass spectrometer for studies of thermal-energy ion-molecule reactions. Technical Report no. 3.

Mie A, Jörntén-Karlsson M, Axelsson B-O, Ray A, Reimann CT. 2007. Enantiomer separation of amino acids by complexation with chiral reference compounds and high-field asymmetric waveform ion mobility spectrometry: preliminary results and possible limitations. Anal Chem 79:2850-2858.

Milloy HB, Crompton RW. 1977. Momentum-transfer cross section for electron-helium collisions in the range 4-12 ev. Phys Rev A 15:1847.

Momoh PO, El-Shall MS. 2008. Gas phase hydration of organic ions. Phys Chem Chem Phys 10:4827.

Myung S, Lee YJ, Moon MH, Taraszka J, Sowell R, Koeniger S, Hilderbrand AE, Valentine SJ, Cherbas L, Cherbas P, Kaufmann TC, Miller DF, Mechref Y, Novotny MV, Ewing MA, Sporleder CR, Clemmer DE. 2003. Development of high-sensitivity ion trap ion mobility spectrometry time-of-flight techniques: a high-throughput nano-lc-ims-tof separation of peptides arising from a drosophila protein extract. Anal Chem 75:5137-5145.

Nazarov EG, Coy SL, Krylov EV, Miller RA, Eiceman GA. 2006. Pressure Effects in Differential Mobility Spectrometry. Anal. Chem. 78: 7697-7706

O'Donnell RM, Sun X, Harrington P de B. 2008. Pharmaceutical applications of ion mobility spectrometry. Trac Trends Anal. Chem. 27:44-53.

Pace CN, Treviño S, Prabhakaran E, Scholtz JM. 2004. Protein structure, stability and solubility in water and other solvents. Philos Trans Royal Soc (London) B Biol Sci 359:1225-1234;.

Poornima CS, Dean PM. 1995. Hydration in drug design. 1. multiple hydrogen-bonding features of water molecules in mediating protein-ligand interactions. J computer-aided mol des 9:500-512.

Poully J-C, Nieuwjaer N, Pierre Schermann J. 2008. Structure and dynamics of molecules of pharmaceutical interest in gas phase and in aqueous phase. Phys. Scr 78:058123.

Prieto M, Yost RA. 2011. Spherical FAIMS: comparison of curved electrode geometries. Int. J Ion Mobil. Spec.14: 61-69

Pringle SD, Giles K, Wildgoose JL, Williams JP, Slade SE, Thalassinos K, Bateman RH, Bowers MT, Scrivens JH. 2007. An investigation of the mobility separation of some peptide and protein ions using a new hybrid quadrupole/travelling wave IMS/oa-ToF instrument. Int. J. Mass Spectrom. 261:1–12.

Pris AD, Mondello FJ, Wroczynski RJ, Murray AJ, Boudries H, Surman CM, Paxon TL. 2009. Improved specific biodetection with ion trap mobility spectrometry (itms): a 10-min, multiplexed, immunomagnetic elisa. Anal Chem 81:9948-9954.

Purves RW, Barnett DA, Ells B, Guevremont R. 2000. Investigation of bovine ubiquitin conformers separated by high-field asymmetric waveform ion mobility spectrometry: cross section measurements using energy-loss experiments with a triple quadrupole mass spectrometer. J Am Soc Mass Spectrom. 11:738-745

Shvartsburg A, Purves RW. 2010., differential ion mobility spectrometry: nonlinear ion transport and fundamentals of faims, crc press, taylor and francis group, boca raton, fl 33487-2742, usa (2009) ISBN 978-1-4200-5106-3 hardcover, 322 pp. J Am Soc Mass Spectrom 21:R3-R3.

Rand KD, Pringle SD, Murphy JP, Fadgen KE, Brown J, Engen JR. 2009. Gas-phase hydrogen/deuterium exchange in a traveling wave ion guide for the examination of protein conformations. Anal Chem 81:10019-10028.

1659 Révész Á, Schröder D, Rokob TA, Havlík M, Dolenský B. 2011. In - flight epimerization of a
1660   *bis* - Tröger base. Angew Chem Int Ed 50:2401-2404.
1661 Roentgen W. 1896. Eine neue art von strahlen 4th ed. Würzburg: Stahel'schen K.B. Hof und
1662   Universitätsbuch und Kunsthandlung.
1663 Ruotolo BT, Giles K, Campuzano I, Sandercock AM, Bateman RH, Robinson CV. 2005. Evidence for
1664   macromolecular protein rings in the absence of bulk water. Science 310:1658-1661.
1665 Ruotolo BT, Gillig KJ, Stone EG, Russell DH. 2002a. Peak capacity of ion mobility mass spectrometry:
1666   separation of peptides in helium buffer gas. J Chromatog B 782:385-392.
1667 Ruotolo BT, Gillig KJ, Stone EG, Russell DH, Fuhrer K, Gonin M, Schultz JA. 2002b. Analysis of
1668   protein mixtures by matrix-assisted laser desorption ionization-ion mobility-orthogonal-time-of-
1669   flight mass spectrometry. Int J Mass Spectrom 219:253-267.
1670 Rus J, Moro D, Sillero JA, Royuela J, Casado A, Estevez-Molinero F, Fernández de la Mora J. 2010.
1671   IMS–MS studies based on coupling a differential mobility analyzer (DMA) to commercial API–
1672   MS systems. Int J Mass Spectrom. 298:30-40
1673 Rutherford E. 1897. The velocity and rate of recombination of the ions of gases exposed to röntgen
1674   radiation. Philosophical Magazine 5: 44:422.
1675 Santos LFA, Iglesias AH, Pilau EJ, Gomes AF, Gozzo FC. 2010. Traveling-wave ion mobility mass
1676   spectrometry analysis of isomeric modified peptides arising from chemical cross-linking. J Am
1677   Soc Mass Spectrom 21:2062-2069.
1678 Schneider BB, Covey TR, Coy SL, Krylov EV, Nazarov EG. 2010a. Planar differential mobility
1679   spectrometer as a pre-filter for atmospheric pressure ionization mass spectrometry. Int J
1680   Mass Spectrom. 298: 45-54
1681 Schneider BB, Covey TR, Coy SL, Krylov EV, Nazarov EG. 2010b. Chemical effects in the separation
1682   process of a differential mobility/mass spectrometer system. Anal Chem 82:1867-1880.
1683 Schneider BB, Covey TR, Coy SL, Krylov EV, Nazarov EG. 2010c. Control of chemical effects in the
1684   separation process of a differential mobility mass spectrometer system Eur J Mass Spectrom
1685   16: 57-71
1686 Schultz SG, Solomon AK. 1961. Determination of the effective hydrodynamic radii of small molecules
1687   by viscometry. J Gen Physiol 44:1189 -1199.
1688 Shelimov KB, Clemmer DE, Hudgins RR, Jarrold MF. 1997. Protein structure *in vacuo*: gas-phase
1689   conformations of bpti and cytochrome c. J Am Chem Soc 119:2240-2248.
1690 Shelimov KB, Jarrold MF. 1997. Conformations, unfolding, and refolding of apomyoglobin in vacuum:
1691   an activation barrier for gas-phase protein folding. J Am Chem Soc 119:2987-2994.
1692 Shvartsburg AA, Clemmer DE, Smith RD. 2010a. Isotopic effect on ion mobility and separation of
1693   isotopomers by high-field ion mobility spectrometry. Anal Chem 82:8047-8051.
1694 Shvartsburg AA, Danielson WF, Smith RD. 2010b. High-resolution differential ion mobility separations
1695   using helium-rich gases. Anal Chem 82:2456-2462.
1696 Shvartsburg AA, Jarrold MF. 1996. An exact hard-spheres scattering model for the mobilities of
1697   polyatomic ions. Chem Phys Lett 261:86-91.
1698 Shvartsburg AA, Mashkevich SV, Baker ES, Smith RD. 2007. Optimization of algorithms for ion
1699   mobility calculations. J Phys Chem A 111:2002-2010.
1700 Shvartsburg AA, Smith RD. 2008. Fundamentals of traveling wave ion mobility spectrometry. Anal
1701   Chem 80:9689-9699.
1702 Shvartsburg AA, Smith RD, Wilks A, Koehl A, Ruiz-Alonso D, Boyle B. 2009a. Ultrafast differential ion
1703   mobility spectrometry at extreme electric fields in multichannel microchips. Anal Chem
1704   81:6489-6495.
1705 Shvartsburg AA, Tang K, Smith RD. 2004. Modeling the resolution and sensitivity of faims analyses. J
1706   Am Soc Mass Spectrom 15:1487-1498.
1707 Shvartsburg AA, Tang K, Smith RD, Holden M, Rush M, Thompson A, Toutoungi D. 2009b. Ultrafast
1708   differential ion mobility spectrometry at extreme electric fields coupled to mass spectrometry.
1709   Anal Chem 81:8048-8053.
1710 Siems WF, Wu C, Tarver EE, Hill HHJ, Larsen PR, McMinn DG. 1994. Measuring the resolving power
1711   of ion mobility spectrometers. Anal Chem 66:4195-4201.
1712 Siu C-K, Guo Y, Saminathan IS, Hopkinson AC, Siu KWM. 2010. Optimization of parameters used in
1713   algorithms of ion-mobility calculation for conformational analyses. J Phys Chem B 114:1204-
1714   1212.
1715 Smith DP, Knapman TW, Campuzano I, Malham RW, Berryman JT, Radford SE, Ashcroft AE. 2009a.
1716   Deciphering drift time measurements from travelling wave ion mobility spectrometry-mass
1717   spectrometry studies. Eur J Mass Spectrom 15:113-130.

Smith RD, Prasad S, Tang K, Manura D, Papanastasiou D. 2009b. Simulation of ion motion in faims through combined use of simion and modified sds. Anal. chem. 81:8749-8757.

Snyder AP, Blyth DA, Parsons JA. 1996. Ion mobility spectrometry as an immunoassay detection technique. J Microbiol Meth 27:81-88.

Snyder AP, Harden CS, Brittain AH, Kim MG, Arnold NS, Meuzelaar HLC. 1993. Portable hand-held gas chromatography/ion mobility spectrometry device. Anal Chem 65:299-306.

Souza Pessôa G de, Pilau EJ, Gozzo FC, Zezzi Arruda MA. 2011. Ion mobility mass spectrometry: an elegant alternative focusing on speciation studies. J. Anal At Spectrom 26:201.

Steiner WE, English WA, Hill HH. 2006.Ion−Neutral Potential Models in Atmospheric Pressure Ion Mobility Time-of-Flight Mass Spectrometry IM(tof)MSJ. Phys. Chem. A. 110:1836-1844

Stolzenburg M, McMurry P. 2008. Equations Governing Single and Tandem DMA Configurations and a New Lognormal Approximation to the Transfer Function. Aerosol Sci. Tech. 42, 421-432Tabrizchi M, Jazan E. 2010. Inverse ion mobility spectrometry. Anal Chem 82:746-750.

Tang K, Shvartsburg AA, Lee H-N, Prior DC, Buschbach MA, Li F, Tolmachev AV, Anderson GA, Smith RD. 2005. High-sensitivity ion mobility spectrometry/mass spectrometry using electrodynamic ion funnel interfaces. Anal Chem 77:3330-3339.

Tang X, Bruce JE, Hill HH. 2006. Characterizing electrospray ionization using atmospheric pressure ion mobility spectrometry. Anal Chem 78:7751-7760.

Taraszka JA, Gao X, Valentine SJ, Sowell RA, Koeniger SL, Miller DF, Kaufman TC, Clemmer DE. 2005. Proteome profiling for assessing diversity: analysis of individual heads of drosophila melanogaster using lc−ion mobility−ms. J Proteome Res 4:1238-1247.

Tarver EE. 2004. External second gate, fourier transform ion mobility spectrometry: parametric optimization for detection of weapons of mass destruction. Sensors 4:1-13.

Thalassinos K, Grabenauer M, Slade SE, Hilton GR, Bowers MT, Scrivens JH. 2009. Characterization of phosphorylated peptides using travelling wave-based and drift cell ion mobility mass spectrometry. Anal Chem 81:248-254.

Thomson JJ. 1903. Conduction of electricity through gases. Nature 69:74-75.

Thomson JJ, Rutherford E. 1896. On the passage of electricity through gases exposed to röntgen rays. Phil Mag Series 5 42:392.

Tuovinen K, Paakkanen H, Hänninen O. 2000. Detection of pesticides from liquid matrices by ion mobility spectrometry. Anal Chim Acta 404:7-17.

Turner RB, Brokenshire JL. 1994. Hand-held ion mobility spectrometers. Trac Trends Anal Chem 13:281-286.

Ude S, Fernández de la Mora J, Thomson BA. 2004. Charge-Induced Unfolding of Multiply Charged Polyethylene Glycol Ions. J. Am. Chem. Soc.126: 12184-12190

Uetrecht C, Rose RJ, Duijn E van, Lorenzen K, Heck AJR. 2010. Ion mobility mass spectrometry of proteins and protein assemblies. Chem Soc Rev 39:1633-1655.

Valentine SJ, Kulchania M, Barnes CAS, Clemmer DE. 2001. Multidimensional separations of complex peptide mixtures: a combined high-performance liquid chromatography/ion mobility/time-of-flight mass spectrometry approach. Int J Mass Spectrom 212:97-109.

Valentine SJ, Stokes ST, Kurulugama RT, Nachtigall FM, Clemmer DE. 2009. Overtone mobility spectrometry: part 2. theoretical considerations of resolving power. J Am Soc Mass Spectrom 20:738-750.

Vautz W, Schwarz L, Hariharan C, Schilling M. 2010. Ion characterisation by comparison of ion mobility spectrometry and mass spectrometry data. Int J Ion Mobil Spec 13:121-129.

Vonderach M, Ehrler OT, Weis P, Kappes MM. 2011. Combining ion mobility spectrometry, mass spectrometry, and photoelectron spectroscopy in a high-transmission instrument. Anal Chem 83:1108-1115.

Wang B, Valentine S, Plasencia M, Raghuraman S, Zhang X. 2010. Artificial neural networks for the prediction of peptide drift time in ion mobility mass spectrometry. BMC Bioinfo 11:182.

Wang Y, Nacson S, Pawliszyn J. 2007. The coupling of solid-phase microextraction/surface enhanced laser desorption/ionization to ion mobility spectrometry for drug analysis. Anal Chim Acta 582:50-54.

Wessel MD, Jurs PC. 1994. Prediction of reduced ion mobility constants from structural information using multiple linear regression analysis and computational neural networks. Anal Chem 66:2480-2487.

Wessel MD, Sutter JM, Jurs PC. 1996. Prediction of reduced ion mobility constants of organic compounds from molecular structure. Anal Chem 68:4237-4243.

1776 Weston DJ, Bateman R, Wilson ID, Wood TR, Creaser CS. 2005. Direct analysis of pharmaceutical
1777   drug formulations using ion mobility spectrometry/quadrupole-time-of-flight mass
1778   spectrometry combined with desorption electrospray ionization. Anal. Chem 77:7572-7580.
1779 Weston DJ. 2010. Ambient ionization mass spectrometry: current understanding of mechanistic
1780   theory; analytical performance and application areas. Analyst 135:661.
1781 Williams JP, Lough JA, Campuzano I, Richardson K, Sadler PJ. 2009a. Use of ion mobility mass
1782   spectrometry and a collision cross-section algorithm to study an organometallic ruthenium
1783   anticancer complex and its adducts with a dna oligonucleotide. Rapid Commun Mass
1784   Spectrom 23:3563-3569.
1785 Williams JP, Bugarcic T, Habtemariam A, Giles K, Campuzano I, Rodger PM, Sadler PJ. 2009b.
1786   Isomer separation and gas-phase configurations of organoruthenium anticancer complexes:
1787   ion mobility mass spectrometry and modeling. J Am Soc Mass Spectrom 20:1119-1122.
1788 Williams JP, Grabenauer M, Holland RJ, Carpenter CJ, Wormald MR, Giles K, Harvey DJ, Bateman
1789   RH, Scrivens JH, Bowers MT. 2010. Characterization of simple isomeric oligosaccharides and
1790   the rapid separation of glycan mixtures by ion mobility mass spectrometry. Int J Mass
1791   Spectrom 298:119-127.
1792 Wren SAC. 2005. Peak capacity in gradient ultra performance liquid chromatography (uplc). J Pharm
1793   Biomed Anal 38:337-343.
1794 Wright P, Alex A, Nyaruwata T, Parsons T, Pullen FS. (2010). Using density functional theory to
1795   rationalise the mass spectral fragmentation of maraviroc and its metabolites. Rapid Commun
1796   in Mass Spectrom, 24: 1025–1031
1797 Wu C, Siems WF, Asbury GR, Hill HH. 1998. Electrospray ionization high-resolution ion mobility
1798   spectrometry−mass spectrometry. Anal Chem 70:4929-4938.
1799 Wyttenbach T, Kemper PR, Bowers MT. 2001. Design of a new electrospray ion mobility mass
1800   spectrometer. Int J Mass Spectrom 212:13-23.
1801 Wyttenbach T, Paizs B, Barran P, Breci L, Liu D, Suhai S, Wysocki VH, Bowers MT. 2003. The effect
1802   of the initial water of hydration on the energetics, structures, and h/d exchange mechanism of
1803   a family of pentapeptides: an experimental and theoretical study. J Am Chem Soc
1804   125:13768-13775.
1805 Zhao W, Bhushan A, Schivo M, Kenyon NJ, Davis CE. 2010. Miniature differential mobility
1806   spectrometry (dms) advances towards portable autonomous health diagnostic systems. In:
1807   Wearable and autonomous biomedical devices and systems for smart environment. Springer
1808   Berlin Heidelberg. Lecture Notes in Electrical Engineering Vol. 75, p. 55-73.
1809   http://dx.doi.org/10.1007/978-3-642-15687-8_3.
1810 Zhou M, Robinson CV. 2010. When proteomics meets structural biology. Trends Biochem Sci 35:522-
1811   529.
1812 Zhu M, Bendiak B, Clowers B, Hill HH. 2009. Ion mobility-mass spectrometry analysis of isomeric
1813   carbohydrate precursor ions. Anal Bioanal Chem 394:1853-1867.
1814 Zolotov YA. 2006. Ion mobility spectrometry. J Anal Chem 61:519-519.
1815
1816